COLLEGE OF
NANOTECHNOLOGY,
SCIENCE, AND ENGINEERING
UNIVERSITY AT ALBANY | STATE UNIVERSITY OF NEW YORK

Mueller Matrix Spectroscopic Ellipsometry based Scatterometry ***of Nanosheet Structures for GAA Transistors using a Hybrid Metrology Approach***

Alain Diebold

March, 2026

FCMN

COLLEGE OF
NANOTECHNOLOGY,
SCIENCE, AND ENGINEERING
UNIVERSITY AT ALBANY | STATE UNIVERSITY OF NEW YORK

Acknowledgements

- Graduate Student Ezra Mel Pasikatan
- Scatterometry Funding from *ONTO Innovations / Discussions, etc.*
  - Andy Antonelli
  - Nick Keller
- Discussions and XRD/XRR with Markus Kuhn of Rigaku
- Samples from TEL -- Dave Hetzer
  - Subhadeep Kal
  - Matthew Rednor

AGENDA

- What is Scatterometry & Requirements for Scatterometry
- 3D Structures, 3D Devices, and Nanoscale Materials
- X-Ray Characterization
- MMSE-Scatterometry
- 3D Nanowire Test Structures
- Conclusions

COLLEGE OF
NANOTECHNOLOGY,
SCIENCE, AND ENGINEERING
UNIVERSITY AT ALBANY | STATE UNIVERSITY OF NEW YORK

Lithography Metrology via Scatterometry

Determine feature shape and dimension changes in a grating test structure with measurements sites for each die in scribe line or in-die

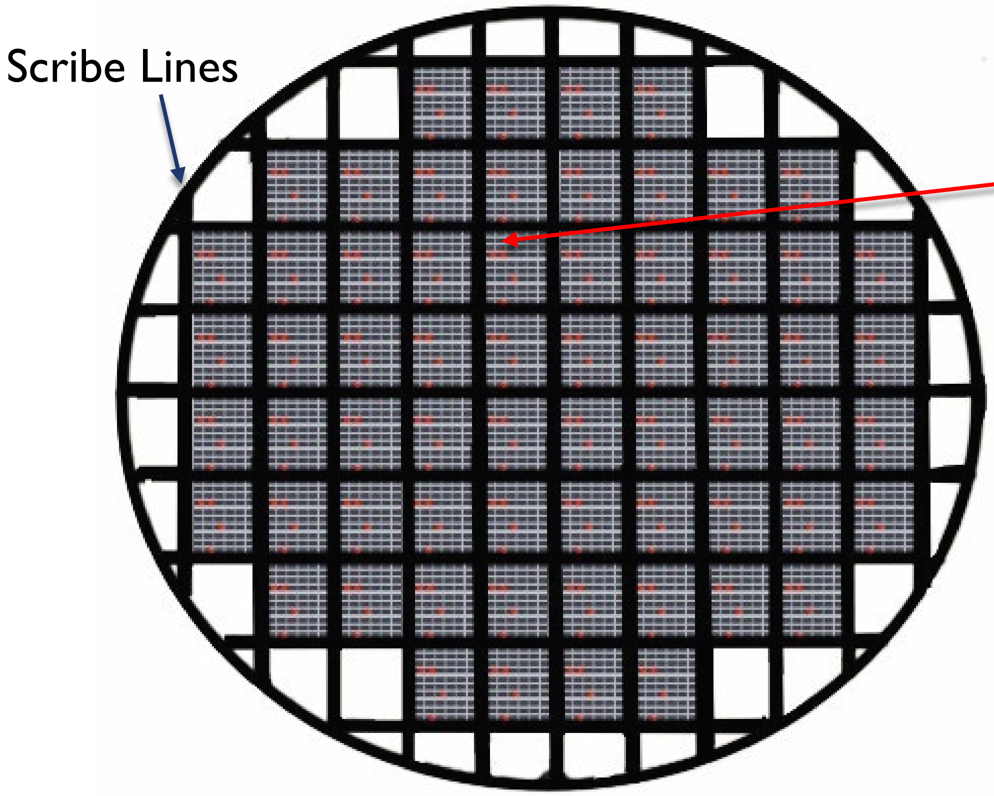

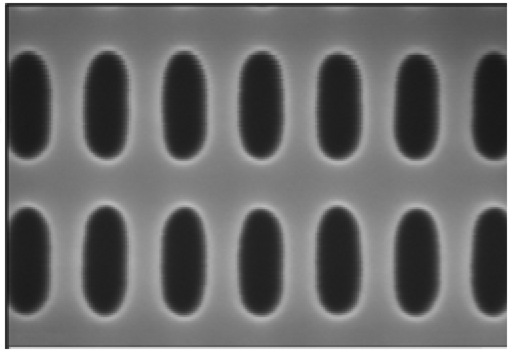

In-Line Ellipsometer

Multiple wafers/hour

Multiple sites/wafer

Capable of Wafer Mapping

What is Scatterometry?

As practiced in the semiconductor industry scatterometry is used to rapidly characterize feature shape and structure of test structures:

- Spectroscopic Ellipsometer – measures grating test structure representative of structure of interest at *multiple areas across the wafer.*
- Model structure & vary a specific set of features using simulation.
- Data analyzed using Rigorous Coupled Wave Analysis solution to Maxwell’s Equations
  - Often done by finding a best match from a library of simulations
  - Sometimes done by finding best fit simulation

What is Needed for Scatterometry ?

- Optical Properties of Fabricated Materials
  - Most process materials have different properties than standard materials –especially dielectric films

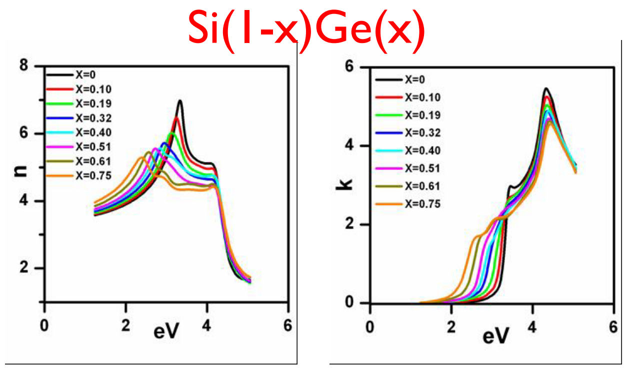

- Reference Measurements to assure film stack and structure shape and dimensions
  - TEM/STEM & XRD/XRR

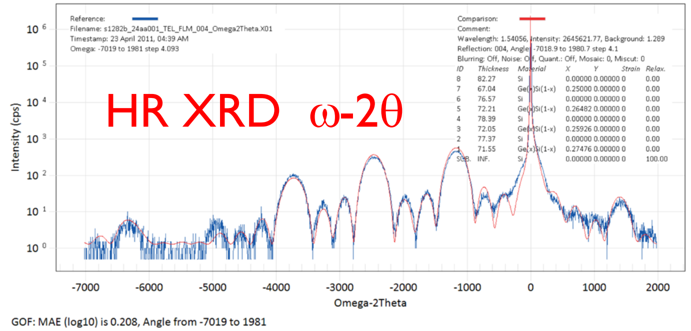

- Ultimately – a Hybrid approach to account for across wafer variation
  - XRD/XRR/XRF & TEM/STEM & Scatterometry

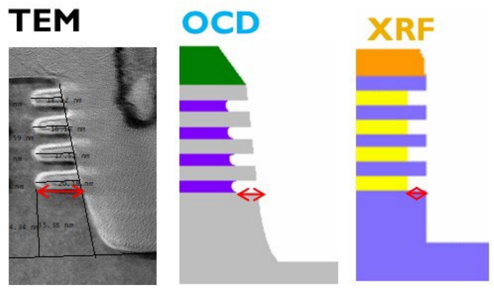

Key Reference for Si(1-x)Ge(x)

- **S. Zollner**
- **Optical Properties and Band Structure of Unstrained and Strained $Si_{1-x}Ge_x$ and $Si_{1-x-y}Ge_xC_y$ alloys**
- **CH 12 in Silicon-Germanium Alloys Growth Properties and Applications**

- Eds. S.T. Pantelides and **S. Zollner**, Vol 15, *Optoelectronic Properties of Semiconductors and Superlattices, Ed. M.O. Manasreh*, (Taylor and Francis, N.Y., 2002), 387.

COLLEGE OF
NANOTECHNOLOGY,
SCIENCE, AND ENGINEERING
UNIVERSITY AT ALBANY | STATE UNIVERSITY OF NEW YORK

AGENDA

- What is Scatterometry & Requirements for Scatterometry
- 3D Structures, 3D Devices, and Nanoscale Materials
- X-Ray Characterization
- MMSE-Scatterometry
- 3D Nanowire Test Structures
- Conclusions

Today 14 nm to < 5 nm
FinFETs to Nanowire/sheet FETs

COLLEGE OF NANOTECHNOLOGY, SCIENCE, AND ENGINEERING
UNIVERSITY AT ALBANY | STATE UNIVERSITY OF NEW YORK

FinFET

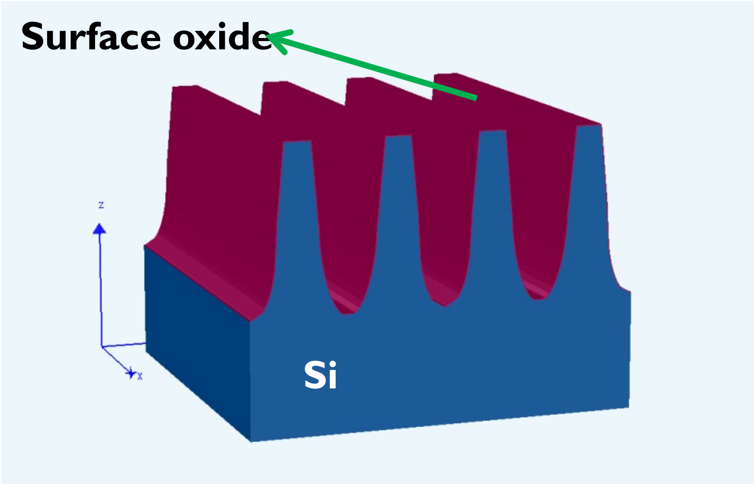

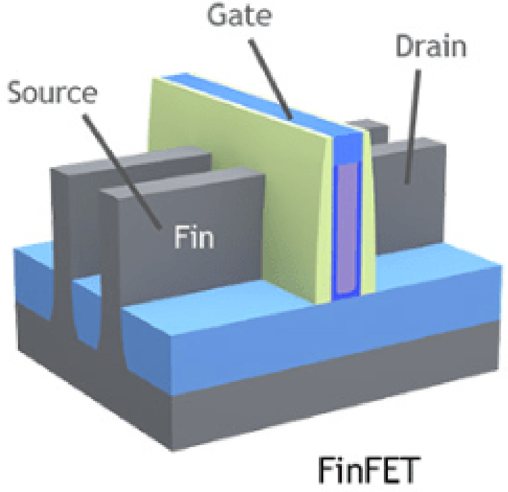

Fins fabricated from a Superlattice of Si/SiGe

NanoWire / NanoSheet FET

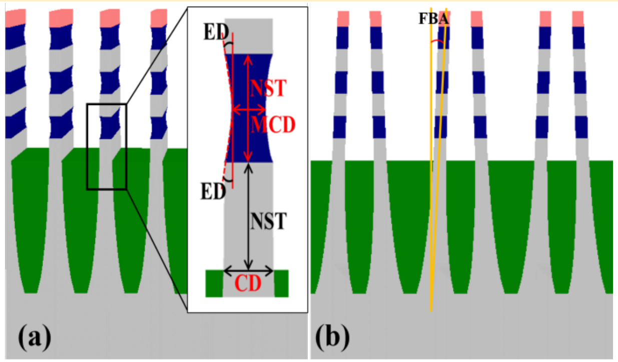

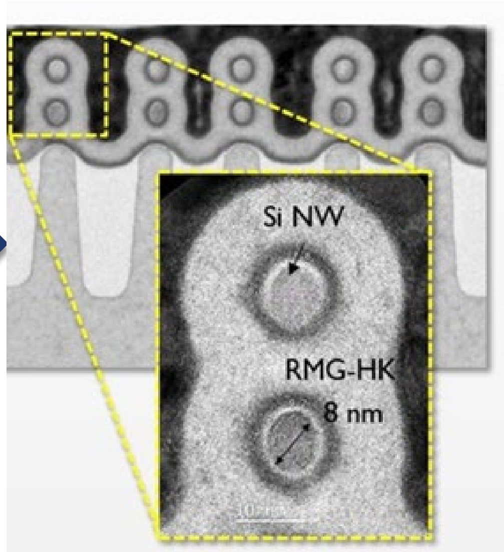

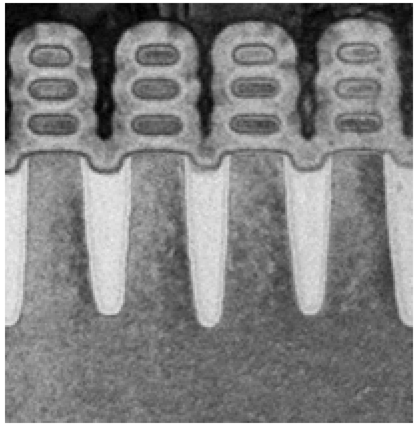

AGENDA

- What is Scatterometry & Requirements for Scatterometry
- 3D Structures, 3D Devices, and Nanoscale Materials
- X-Ray Characterization (Intro to Pseudomorphic $Si_{1-x}Ge_x$)
- MMSE-Scatterometry
- 3D Nanowire Test Structures
- Conclusions

Strained Silicon - Germanium

Silicon and Germanium lattice constants differ by more than 4 %.

$Si_{1-x}Ge_x$ has a larger lattice than that of Silicon

$Si_{1-x}Ge_x$ undergoes bi-axial stress to match Silicon's in-plane lattice.

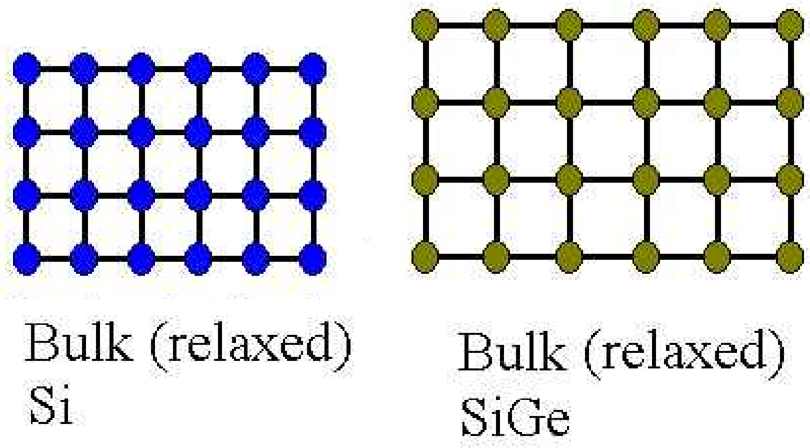

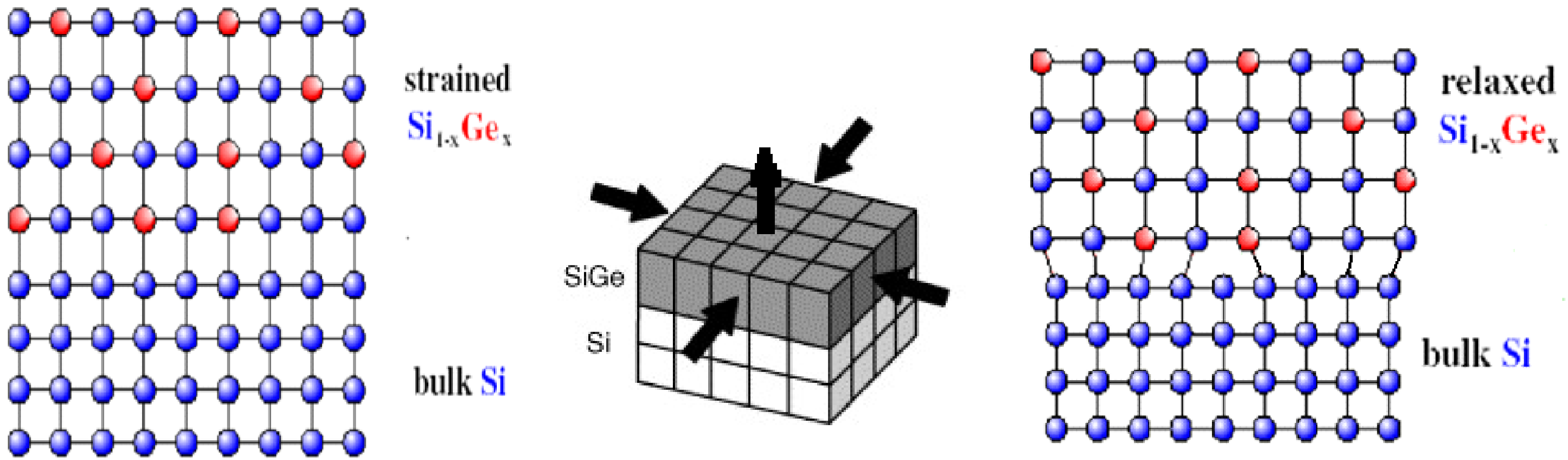

http://www.aip.org/tip/INPHFA/vol-8/iss-3/p22.pdf
http://ars.sciencedirect.com/content/image/1-s2.0-S0167572905000464-gr4.jpg
D.J. Paul, *Physics World* 13, pp27-32 (February 2000)

Determining the Refractive Index (Dielectric Function)

- First we consider a single layer of $Si_{1-x}Ge_x$ on Si

Superlattice Effects on XRD

- Superlattice structure results in diffraction from main SiGe Peak
- Si/SiGe Bilayer can be considered a large unit cell

$$F_{hk\ell} = \sum_{j=1}^{N} f_j e^{[-2\pi i(hx_j+ky_j+\ell z_j)]},$$

Single Unit Cell

$$F_H = \sum_j^N f_j \exp(-2\pi \mathbf{H}.\mathbf{r}_j)$$

Large Unit Cell Structure Factor

004 $\omega - 2\theta$ scan

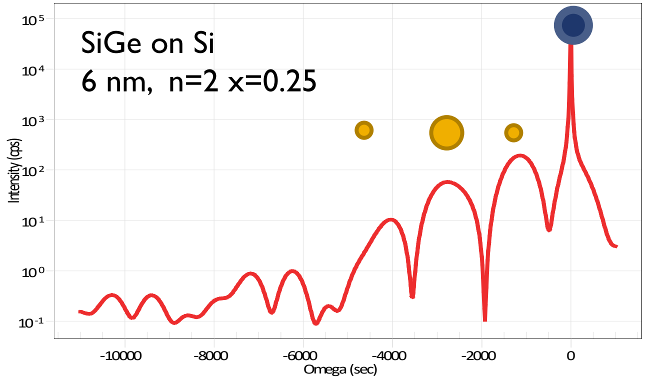

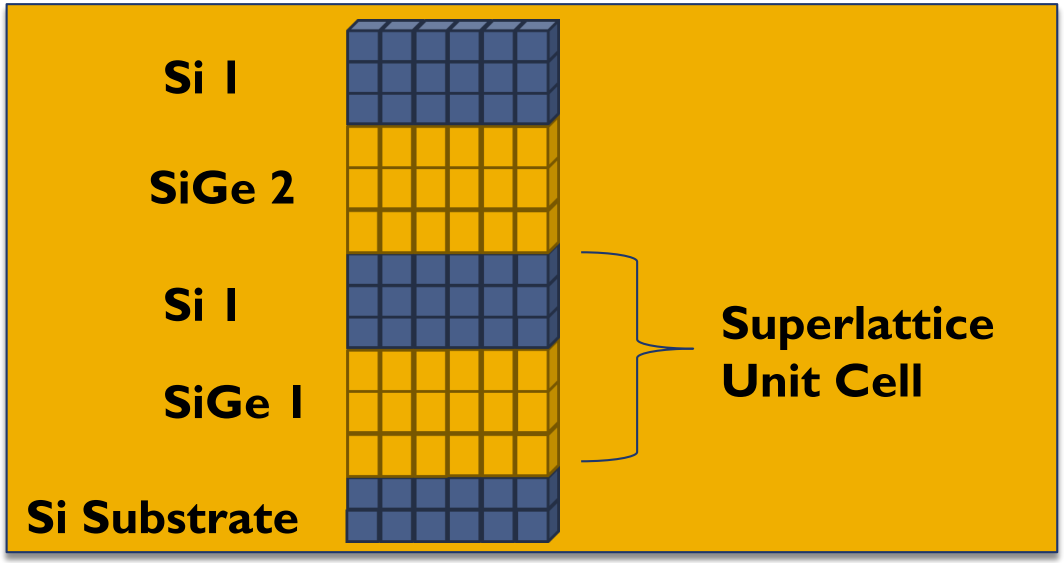

RSM Schematic (Strained Condition)

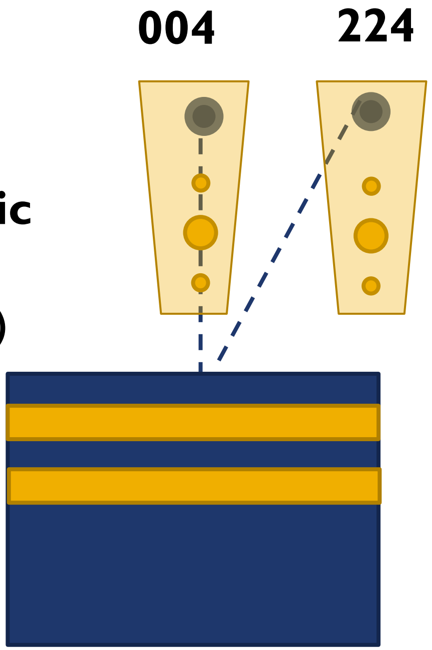

Fewster, P. F. Superlattices. In *X-Ray and Neutron Dynamical Diffraction:Theory and Applications*; 1996; https://doi.org/10.1007/978-1-4615-5879-8_20.

XRD $\omega - 2\theta$: Thickness & Composition Results

- Scanning $\omega - 2\theta$ around Si (004) shows SiGe peak at expected angular offset
- Two additional peaks are due to the superlattice effect (repeating Si/SiGe layers)

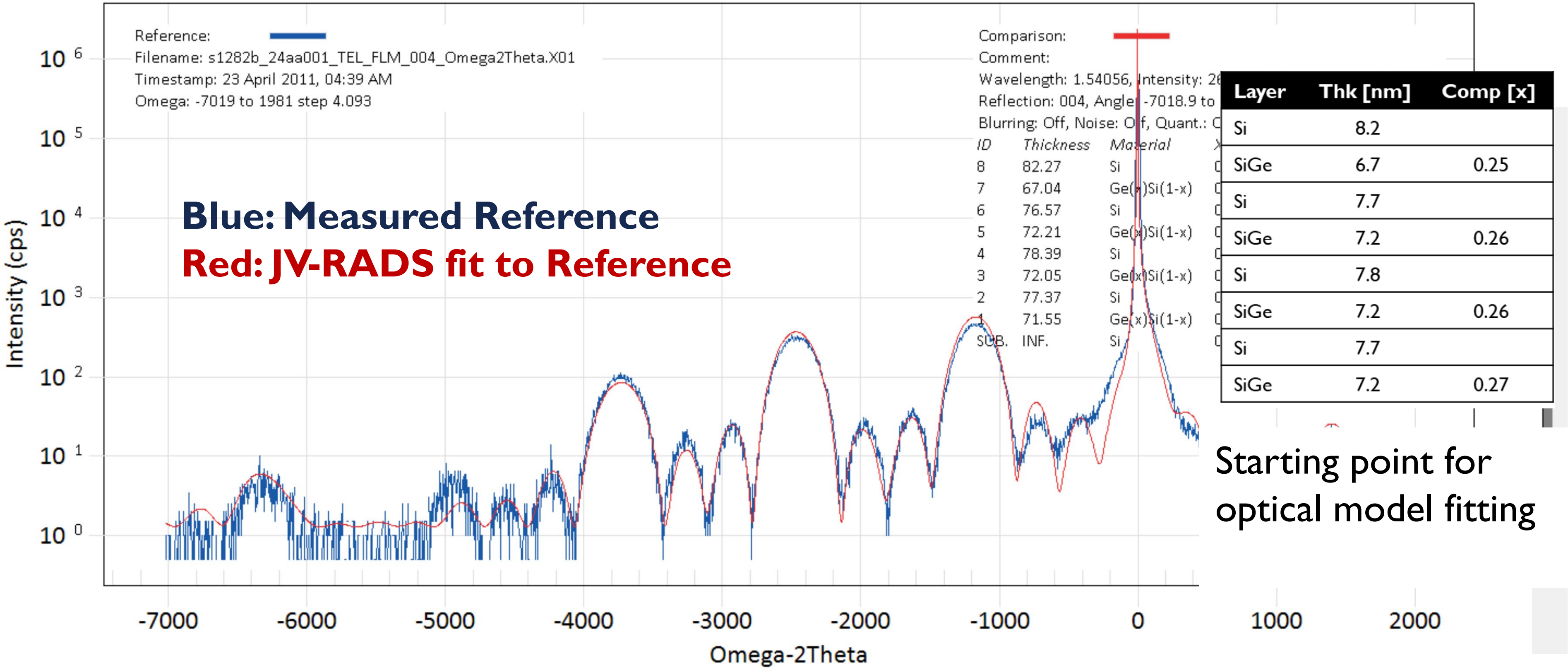

Layer	Thk [nm]	Comp [x]
Si	8.2	
SiGe	6.7	0.25
Si	7.7	
SiGe	7.2	0.26
Si	7.8	
SiGe	7.2	0.26
Si	7.7	
SiGe	7.2	0.27

Starting point for optical model fitting

GOF: MAE (log10) is 0.208, Angle from -7019 to 1981

COLLEGE OF
NANOTECHNOLOGY,
SCIENCE, AND ENGINEERING
UNIVERSITY AT ALBANY | STATE UNIVERSITY OF NEW YORK

8X superlattice Film Variation

Average HR-XRD Layer Thickness

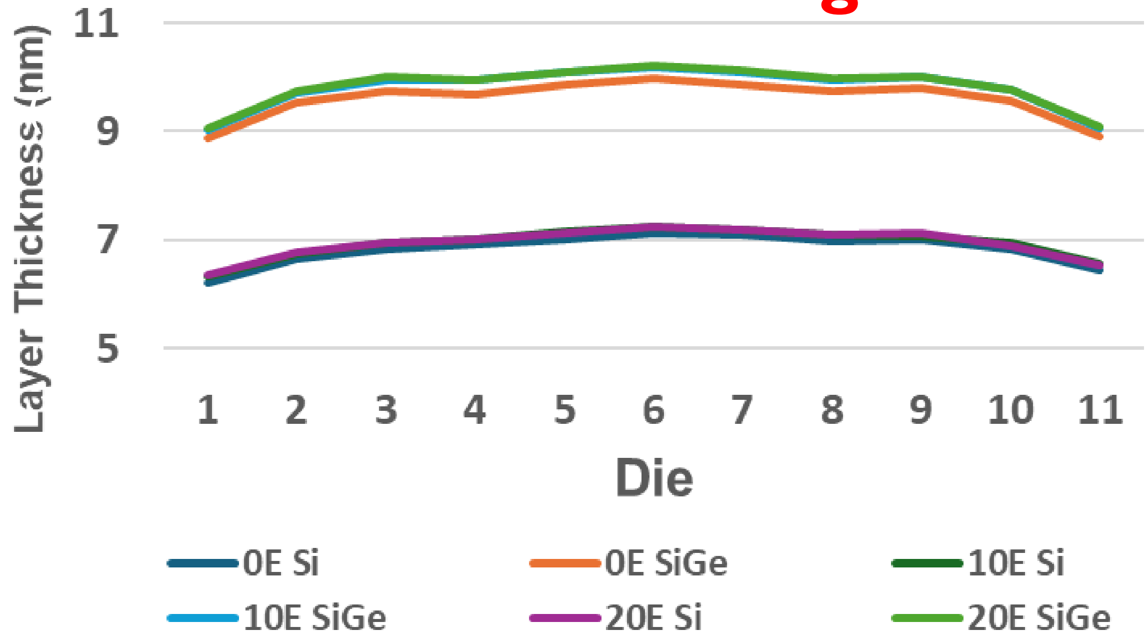

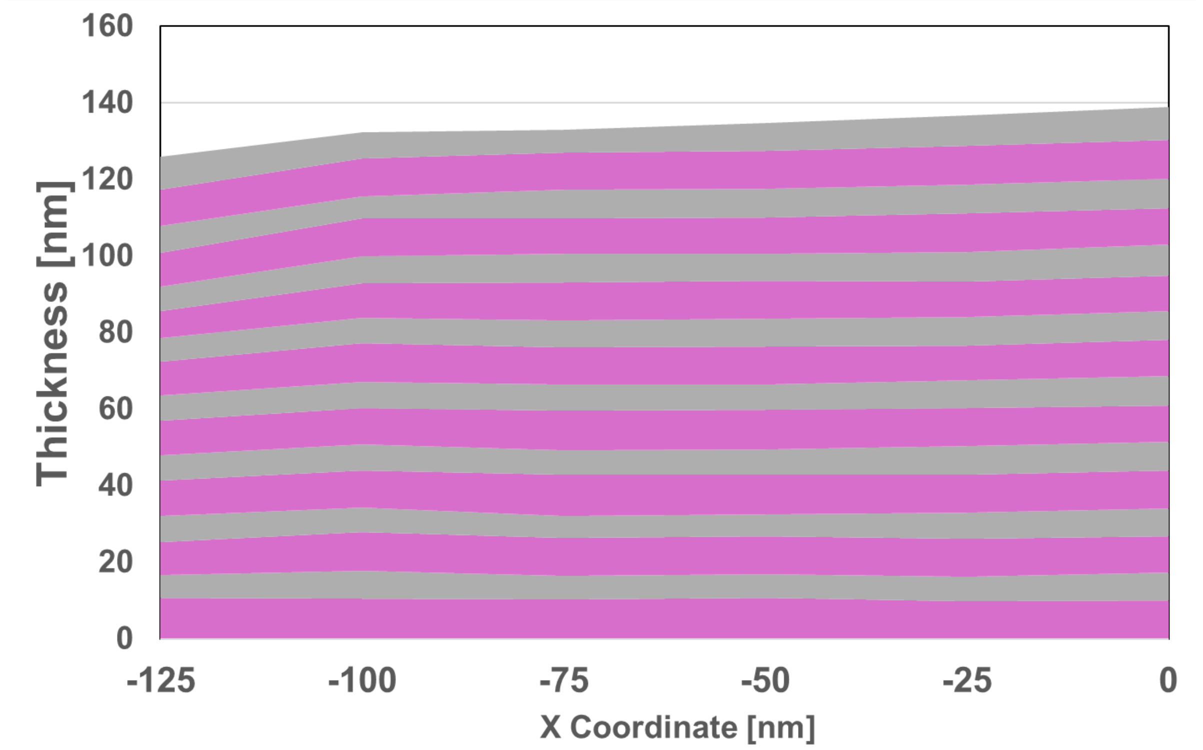

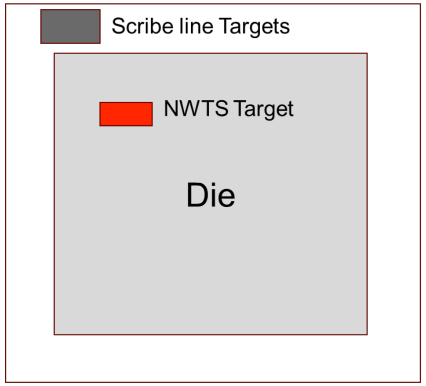

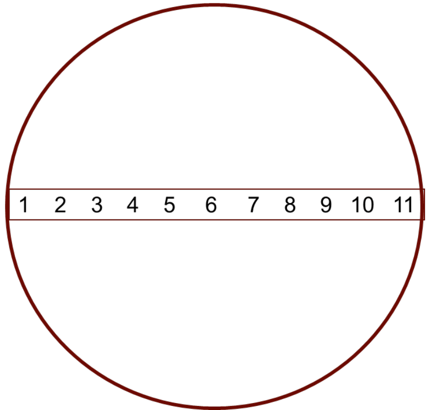

Magnified view of area for Dies 1 to 6

Reciprocal Space Maps: Strain / Relaxation and Tilts

- A scan around a reciprocal lattice point (rlp) provides good interpretation of the structure of a material
- Any relaxation/tilt on the layers with respect to the substrate is shown as a peak shift away from the substrate peak.

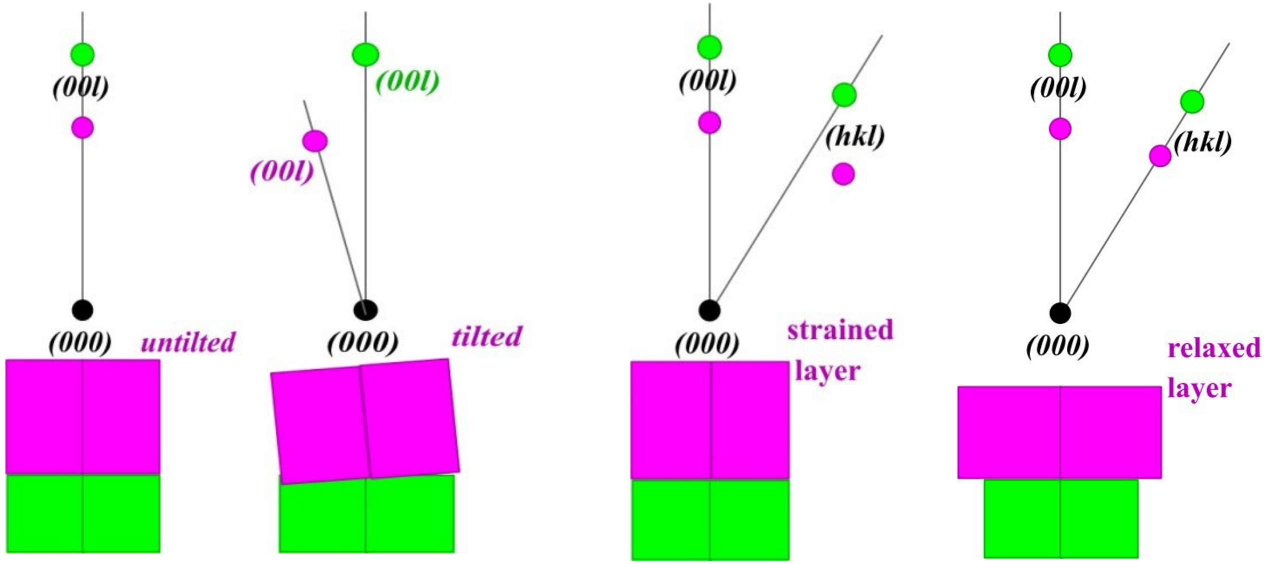

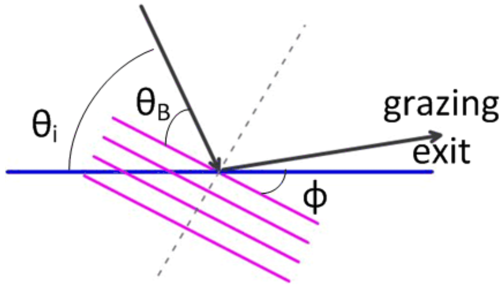

Grazing Exit 224 $\phi = \sim 35.3°$

Symmetric scans to determine tilt of the layer

Asymmetric scans to determine relaxation in the layer

- Grazing Incidence $\theta_i = \theta_B - \varphi$
- Grazing Exit $\theta_i = \theta_B + \varphi$

(7) B. K. Tanner (2005)

Epilayer vs Superlattice RSM

- No relaxation of superlattice layers

	Single SiGe Epilayer on Si X=0.23 52.9 nm	Superlattice 4 Layer Si/SiGe X~0.25 6 nm	Superlattice 8 Layer Si/SiGe X~0.25 < 10 nm
224 RSM	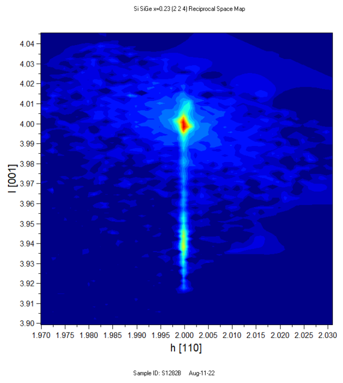	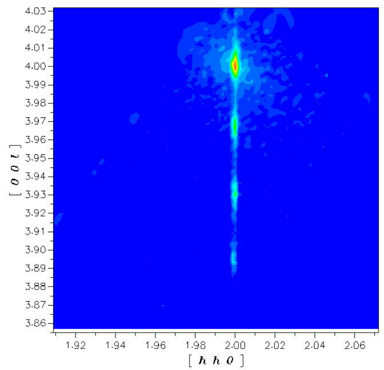	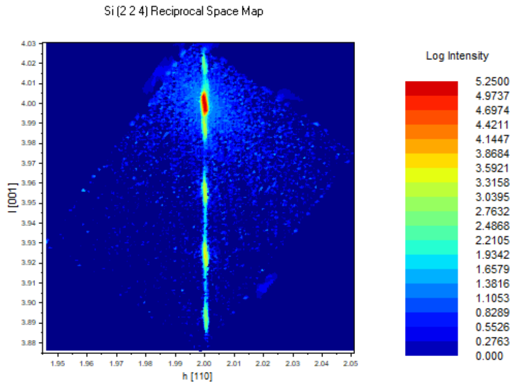
004 RSM	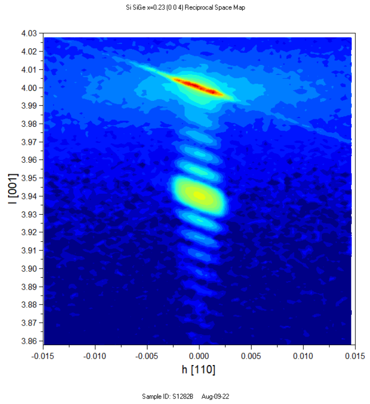	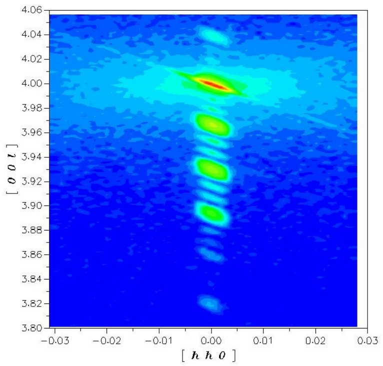	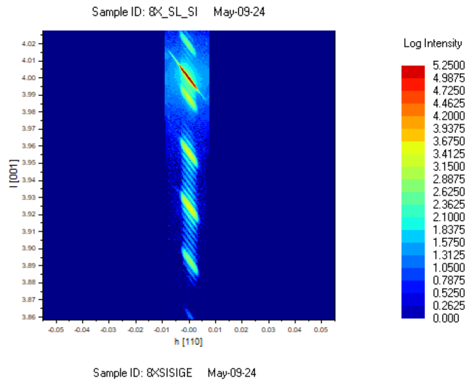

Superlattice & Elastic Model

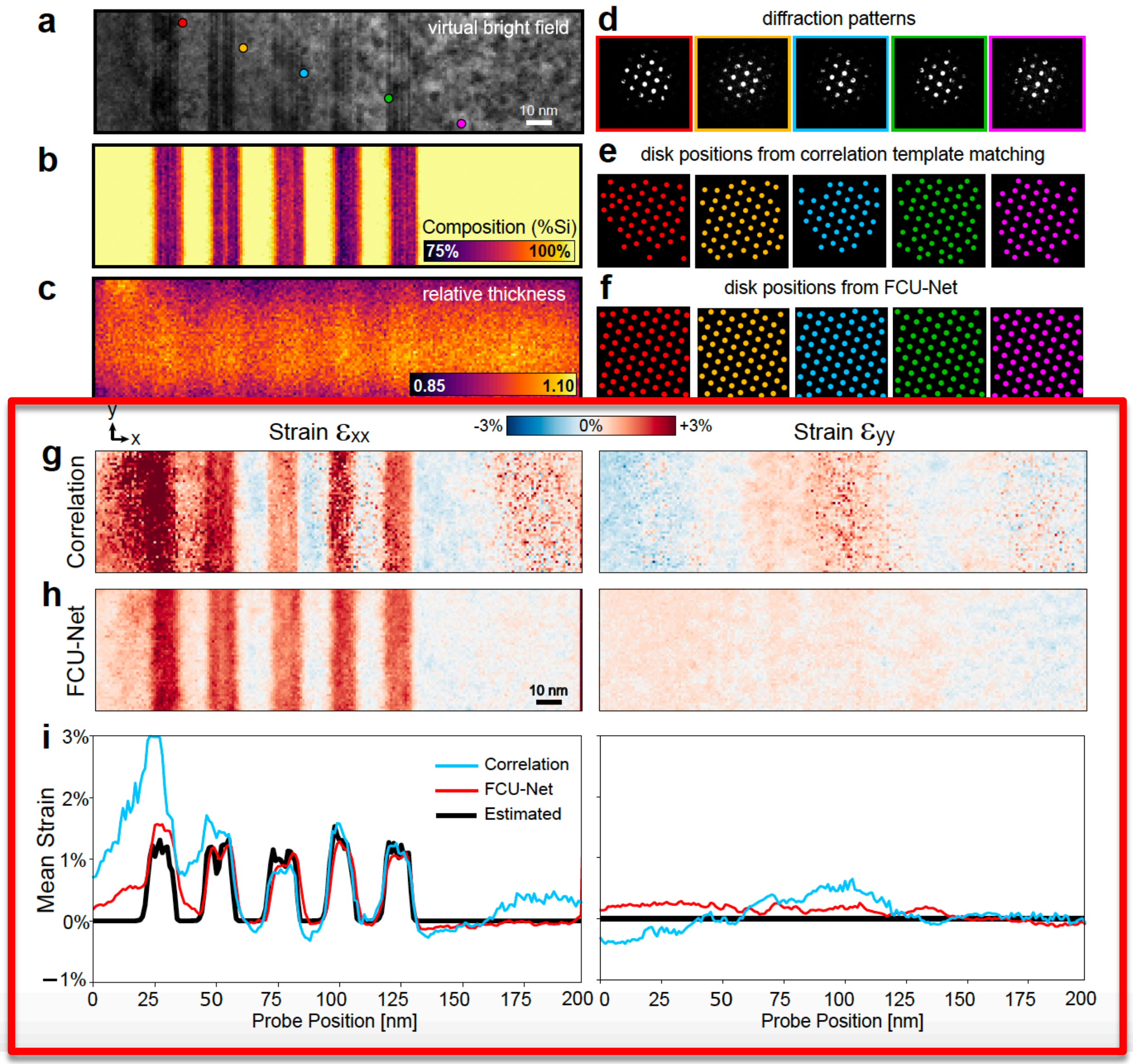

Analysis of experimental CBED strain data using *(Fourier-space complex U net (FCU-Net) deep neural network*

X direction is perpendicular to the layer interfaces

Si/Si(1-x)Ge(x) with x=0.13 (?). Here, strain refers difference from Si lattice.

Munshi, J., *et al.* Disentangling multiple scattering with deep learning: application to strain mapping from electron diffraction patterns. *npj Comput Mater* **8**, 254 (2022). https://doi.org/10.1038/s41524-022-00939-9

XRD/XRR as a Reference Measurement for many layer superlattices ??

- Reference Measurements for Si(1-x)Ge(x)/Si superlattice spectroscopic ellipsometry
  - ω-2θ coupled scans and RSM limited to < 32 layers for transistor stacks – see specifics in J. Micro/Nanopattern. Mater. Metrol. 23, (2024), 044004.
  - Need multiple TEM/STEM measurements per wafer
- For Nanowire test structures (next part of presentation), the SiN hard mask roughness limits ellipsometery measurement of Si(1-x)Ge(x)/Si superlattice

AGENDA

- What is Scatterometry & Requirements for Scatterometry
- 3D Structures, 3D Devices, and Nanoscale Materials
- X-Ray Characterization
- MMSE-Scatterometry
- 3D Nanowire Test Structures
- Conclusions

Scatterometry / Ellipsometry of Grating Structures

- Inline optical metrology tool for critical dimension (CD) measurement for advanced process control. Fast, accurate & non-destructive.
- Diffraction from a periodic grating.
- **Optical simulator is used to generate the optical response for the structure of interest (Forward problem) and regression based or library based approach is used to extract the feature dimensions/additional information (Reverse problem).**

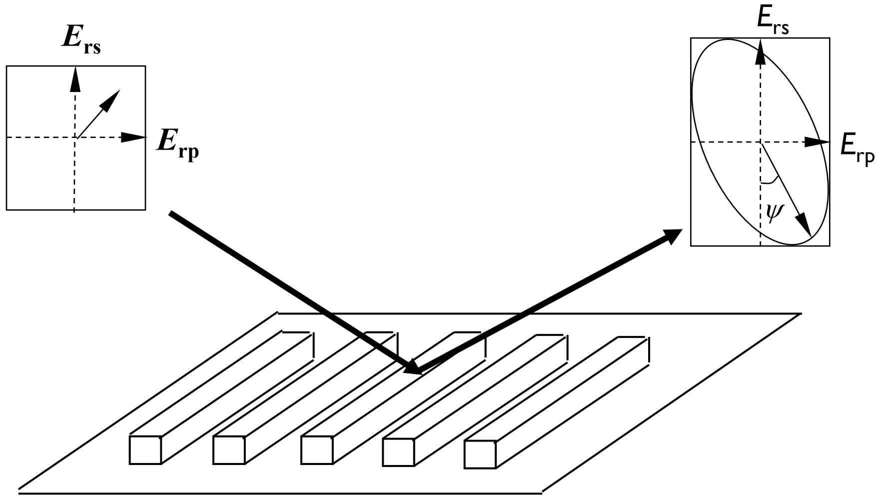

$$\tilde{N} = n + ik \qquad \tilde{N}^2 = \tilde{\varepsilon} = \varepsilon_1 + i\varepsilon_2$$

Optical Response

$$\tan\Psi e^{j\Delta} = \frac{R^p}{R^s}$$

Ellipsometric Response

$$\begin{pmatrix} S_{0,out} \\ S_{1,out} \\ S_{2,out} \\ S_{3,out} \end{pmatrix} = \begin{pmatrix} M_{11} & M_{12} & M_{13} & M_{14} \\ M_{21} & M_{22} & M_{23} & M_{24} \\ M_{31} & M_{32} & M_{33} & M_{34} \\ M_{41} & M_{42} & M_{43} & M_{44} \end{pmatrix} \begin{pmatrix} S_{0,in} \\ S_{1,in} \\ S_{2,in} \\ S_{3,in} \end{pmatrix}$$

Mueller Response

$$S = \begin{bmatrix} s_0 \\ s_1 \\ s_2 \\ s_3 \end{bmatrix} = \begin{bmatrix} I_x + I_y \\ I_x - I_y \\ I_{\pi/4} - I_{-\pi/4} \\ I_{LCP} - I_{RCP} \end{bmatrix}$$

Ellipsometry

$$\frac{r_{pp}}{r_{ss}} = \tan\Psi e^{i\Delta}$$

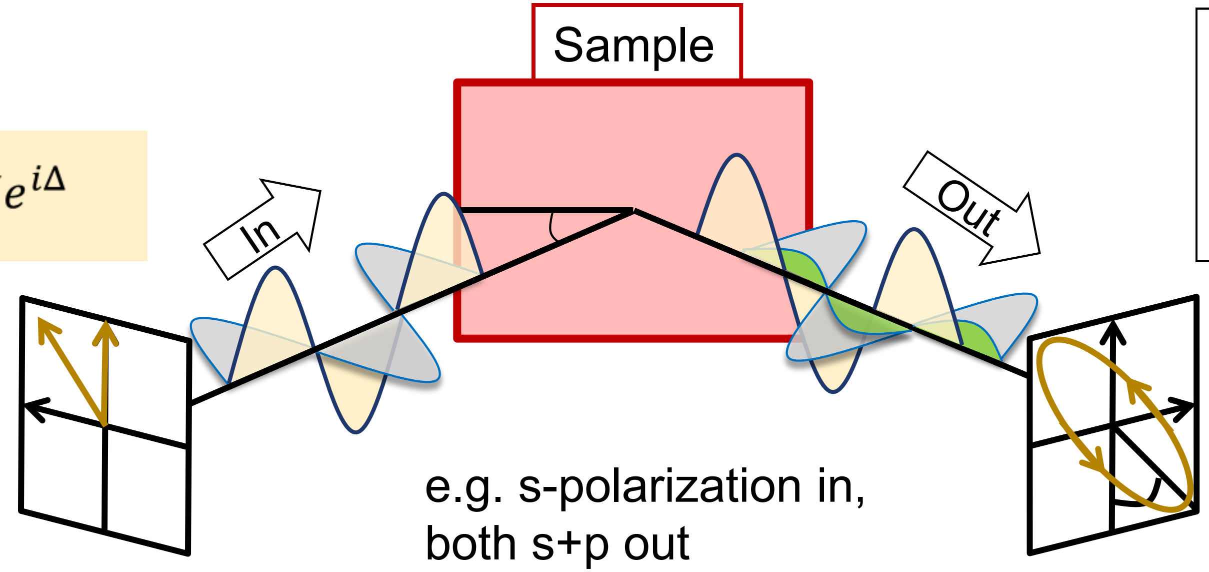

Cross
Standard
Polarization Response

p ⟶ p+s

s ⟶ s+p

$$S = \begin{bmatrix} s_0 \\ s_1 \\ s_2 \\ s_3 \end{bmatrix} = \begin{bmatrix} I_x + I_y \\ I_x - I_y \\ I_{\pi/4} - I_{-\pi/4} \\ I_{LCP} - I_{RCP} \end{bmatrix}$$

- Isotropic samples
  - Refractive indices of thin films lack spatial dependence
  - Thus, no azimuthal dependence or cross-polarization
- Anisotropic structures
  - Patterned surfaces result in spatially varying refractive indices
  - Thus, azimuthal dependence reflects sample symmetry

$$\begin{pmatrix} S_{0,out} \\ S_{1,out} \\ S_{2,out} \\ S_{3,out} \end{pmatrix} = \begin{pmatrix} M_{11} & M_{12} & M_{13} & M_{14} \\ M_{21} & M_{22} & M_{23} & M_{24} \\ M_{31} & M_{32} & M_{33} & M_{34} \\ M_{41} & M_{42} & M_{43} & M_{44} \end{pmatrix} \begin{pmatrix} S_{0,in} \\ S_{1,in} \\ S_{2,in} \\ S_{3,in} \end{pmatrix}$$

COLLEGE OF NANOTECHNOLOGY, SCIENCE, AND ENGINEERING
UNIVERSITY AT ALBANY | STATE UNIVERSITY OF NEW YORK

Dual Rotating Compensator Ellipsometer (RC2)

$$S=\begin{bmatrix} s_0 \\ s_1 \\ s_2 \\ s_3 \end{bmatrix}=\begin{bmatrix} I_x+I_y \\ I_x-I_y \\ I_{\pi/4}-I_{-\pi/4} \\ I_{LCP}-I_{RCP} \end{bmatrix}$$

Stokes Vector

System Mueller Matrix

$$\begin{pmatrix} S_{0,out} \\ S_{1,out} \\ S_{2,out} \\ S_{3,out} \end{pmatrix}=\begin{pmatrix} M_{11} & M_{12} & M_{13} & M_{14} \\ M_{21} & M_{22} & M_{23} & M_{24} \\ M_{31} & M_{32} & M_{33} & M_{34} \\ M_{41} & M_{42} & M_{43} & M_{44} \end{pmatrix}\begin{pmatrix} S_{0,in} \\ S_{1,in} \\ S_{2,in} \\ S_{3,in} \end{pmatrix}$$

Rotation Mueller Matrix

$$RM\ \begin{bmatrix} 1 & 0 & 0 & 0 \\ 0 & \cos 2\alpha & \sin 2\alpha & 0 \\ 0 & -\sin 2\alpha & \cos 2\alpha & 0 \\ 0 & 0 & 0 & 1 \end{bmatrix}$$

Laboratory Ellipsometer
Great for All Types of Samples

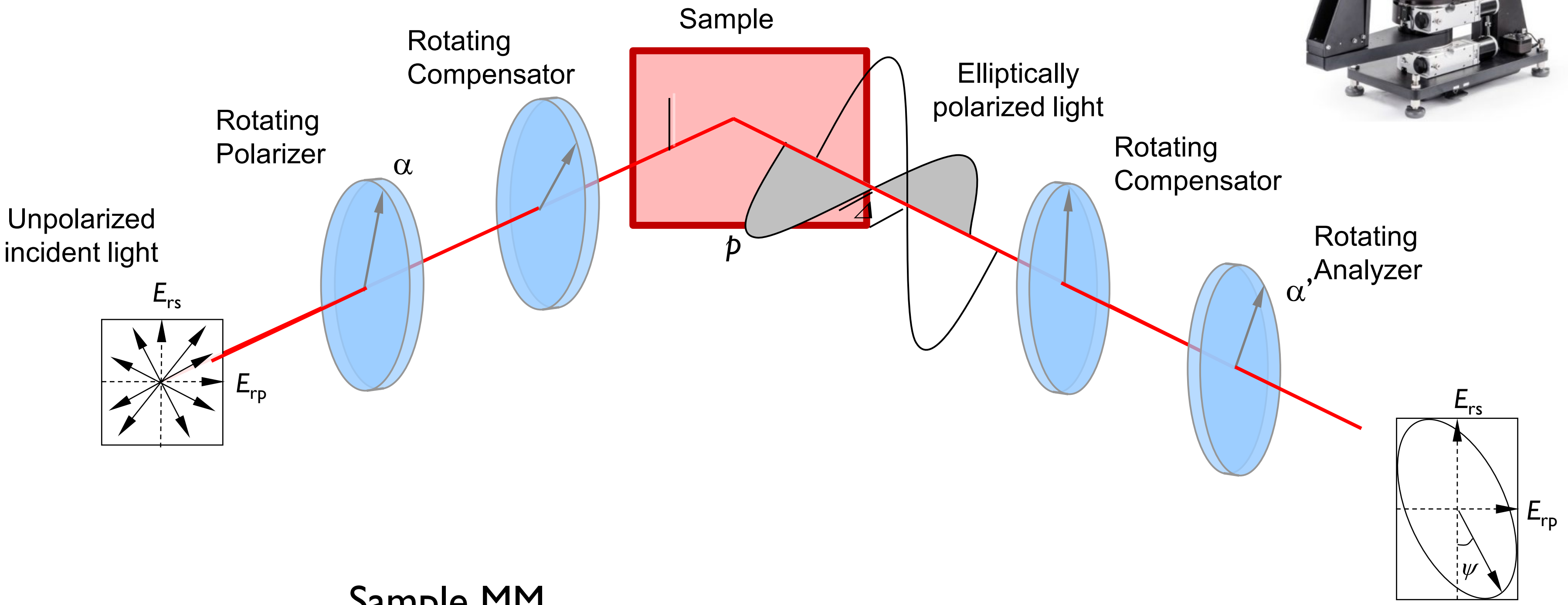

Sample MM

$$\begin{pmatrix} S_{0,in} \\ S_{1,in} \\ S_{2,in} \\ S_{3,in} \end{pmatrix}\ RM\ \frac{1}{2}\begin{bmatrix} 1 & 1 & 0 & 0 \\ 1 & 1 & 0 & 0 \\ 0 & 0 & 0 & 0 \\ 0 & 0 & 0 & 0 \end{bmatrix}\ RM\ \begin{bmatrix} 1 & 0 & 0 & 0 \\ 0 & 1 & 0 & 0 \\ 0 & 0 & \cos\delta & \sin\delta \\ 0 & 0 & -\sin\delta & \cos\delta \end{bmatrix}\begin{pmatrix} M_{11} & M_{12} & M_{13} & M_{14} \\ M_{21} & M_{22} & M_{23} & M_{24} \\ M_{31} & M_{32} & M_{33} & M_{34} \\ M_{41} & M_{42} & M_{43} & M_{44} \end{pmatrix}\begin{bmatrix} 1 & 0 & 0 & 0 \\ 0 & 1 & 0 & 0 \\ 0 & 0 & \cos\delta & \sin\delta \\ 0 & 0 & -\sin\delta & \cos\delta \end{bmatrix}\ RM\ \frac{1}{2}\begin{bmatrix} 1 & 1 & 0 & 0 \\ 1 & 1 & 0 & 0 \\ 0 & 0 & 0 & 0 \\ 0 & 0 & 0 & 0 \end{bmatrix}\ RM = \begin{pmatrix} S_{0,out} \\ S_{1,out} \\ S_{2,out} \\ S_{3,out} \end{pmatrix}$$

Mueller Matrix Basics

Post-normalization

Isotropic
Anisotropic, general
Anisotropic, grating

$$M = \begin{pmatrix} M_{11} & M_{12} & M_{13} & M_{14} \\ M_{21} & M_{22} & M_{23} & M_{24} \\ M_{31} & M_{32} & M_{33} & M_{34} \\ M_{41} & M_{42} & M_{43} & M_{44} \end{pmatrix} = \begin{pmatrix} 1 & -N - \alpha_{sp} & C_{sp} + \zeta_1 & S_{sp} + \zeta_2 \\ -N - \alpha_{ps} & 1 - \alpha_{sp} - \alpha_{ps} & -C_{sp} + \zeta_1 & -S_{sp} + \zeta_2 \\ C_{ps} + \xi_1 & -C_{ps} + \xi_1 & C_{pp} + \beta_1 & S_{pp} + \beta_2 \\ -S_{ps} + \xi_2 & S_{ps} + \xi_2 & -S_{pp} - \beta_2 & C_{pp} - \beta_1 \end{pmatrix}$$

- Matrix contains complete optical response of a sample
- Symmetry reduces number of independent elements
- 15 distinct elements in general

$$D = 1 + \tan^2(\psi_{pp}) + \tan^2(\psi_{ps}) + \tan^2(\psi_{sp})$$

$$N = \frac{1 - \tan^2(\psi_{pp}) - \tan^2(\psi_{ps}) - \tan^2(\psi_{sp})}{D}$$

$$C_{ij} = \frac{2\tan(\psi_{ij})\ \cos\Delta_{ij}}{D}$$

$$S_{ij} = \frac{2\tan(\psi_{ij})\ \sin\Delta_{ij}}{D}$$

$$\alpha_{ij} = \frac{2\tan^2(\psi_{ij})}{D}$$

$$\zeta_i = \frac{D\left(C_{ps}^2 + S_{ps}^2(-1)^{i+1 \bmod 2}\right)}{2}$$

$$\xi_i = \frac{D\left(C_{sp}^2 + S_{sp}^2(-1)^{i+1 \bmod 2}\right)}{2}$$

$$\beta_i = \frac{D\left(C_{sp}C_{ps} + S_{sp}S_{ps}(-1)^{i+1 \bmod 2}\right)}{2}$$

Mueller Matrix Basics

Symmetric (Ideal) Grating

$$M = \begin{pmatrix} M_{11} & M_{12} & M_{13} & M_{14} \\ M_{21} & M_{22} & M_{23} & M_{24} \\ M_{31} & M_{32} & M_{33} & M_{34} \\ M_{41} & M_{42} & M_{43} & M_{44} \end{pmatrix} = \begin{pmatrix} 1 & -N-\alpha_{sp} & C_{sp}+\zeta_1 & S_{sp}+\zeta_2 \\ -N-\alpha_{ps} & 1-\alpha_{sp}-\alpha_{ps} & -C_{sp}+\zeta_1 & -S_{sp}+\zeta_2 \\ C_{ps}+\xi_1 & -C_{ps}+\xi_1 & C_{pp}+\beta_1 & S_{pp}+\beta_2 \\ -S_{ps}+\xi_2 & S_{ps}+\xi_2 & -S_{pp}-\beta_2 & C_{pp}-\beta_1 \end{pmatrix}$$

M13+M31 and M14-M41 non zero = sample asymmetry

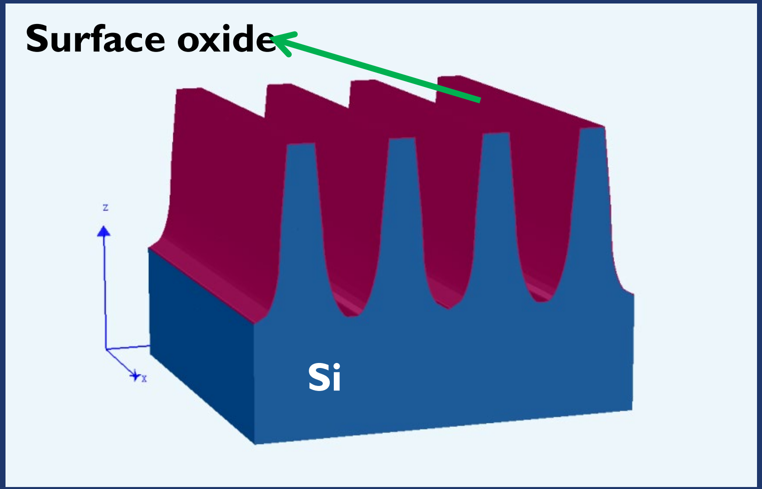

M_{11}	M_{12}	M_{13}	M_{14}
M_{12}	M_{22}	M_{23}	M_{24}
$-M_{13}$	$-M_{23}$	M_{33}	M_{34}
M_{14}	M_{24}	$-M_{34}$	M_{44}

Rigorous Coupled Wave Approximation (RCWA)

- Approximate full Fourier series for dielectric function

$$\varepsilon(x) = \sum_{n=-N}^{N} \varepsilon_n e^{i2\pi nx/\Lambda}$$

- Slice structure into stack of layers, coefficients determined:

$$\varepsilon_{n=0} = \varepsilon_{line} d/\Lambda + \varepsilon_{space}(1 - d/\Lambda) \qquad \varepsilon_{n\neq 0} = (\varepsilon_{line} - \varepsilon_{space})\sin(n\pi d/\Lambda)/n\pi$$

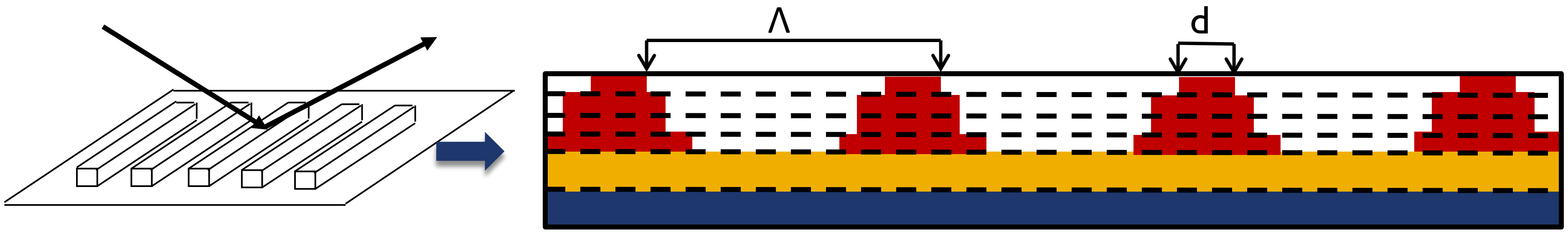

- Solve Maxwell's equations for incident TE and TM polarized waves

$$H = \left(\frac{i}{\omega\mu}\right)\nabla \times E \qquad E = \left(\frac{i}{\omega\mu n^2}\right)\nabla \times H$$

- Equations cast in Matrix Form

Formulation of Rigorous Coupled-Wave Approximation (RCWA)

- Semi – Analytical Form of Maxwell’s Equations in Fourier Space
- Transform only in-plane (x and y) and have a uniform layer in z
- Transform Maxwell’s equations into a computer solvable matrix form
- Alternate name: Transfer matrix method with a plane wave basis

See **EM Possible** - Implementation of 3D RCWA in MATLAB

Must Know Optical Properties of the Layers

Reference Method – HR-XRD (example $Si_{1-x}Ge_x/Si$)

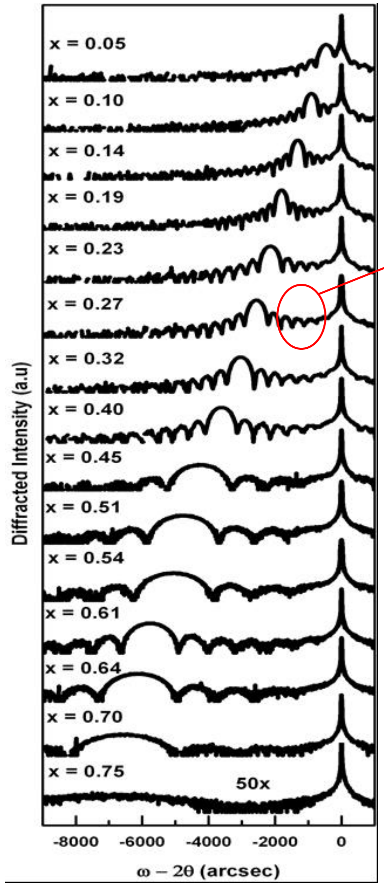

$$Thickness = \frac{\lambda}{2\Delta\omega_{fringes}\cos\theta_B}$$

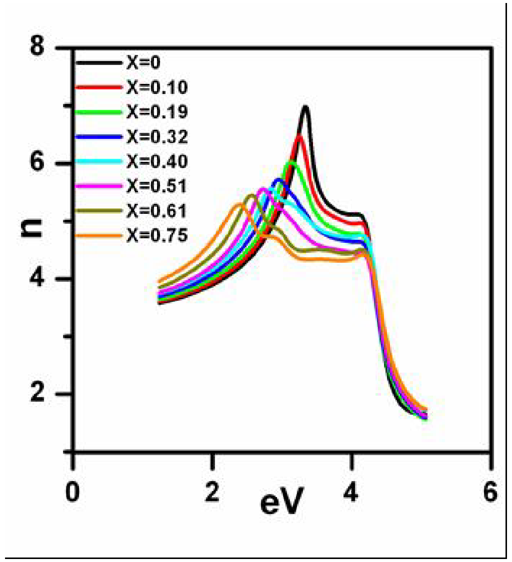

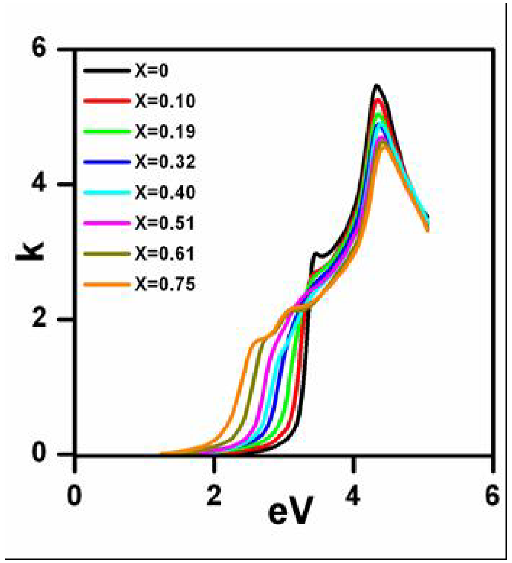

J. Appl. Phys. 112, 053519 (2012)

COLLEGE OF
NANOTECHNOLOGY,
SCIENCE, AND ENGINEERING
UNIVERSITY AT ALBANY | STATE UNIVERSITY OF NEW YORK

Optical Properties of SiN Hard Mask

- SiN_x film optical properties are dependent on process conditions
- Deposited SiN_x film on Si substrate deposited at the same process conditions superlattice stack
- Derived material file based on XRR thickness and SE data

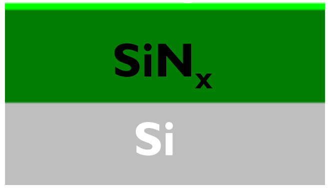

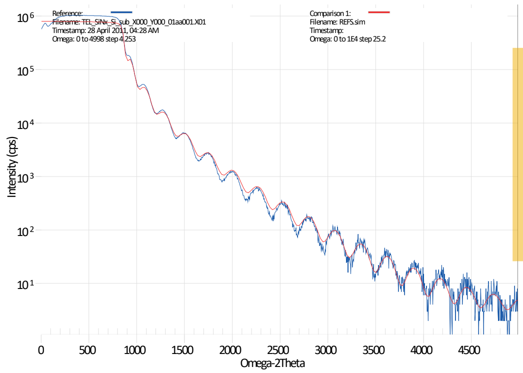

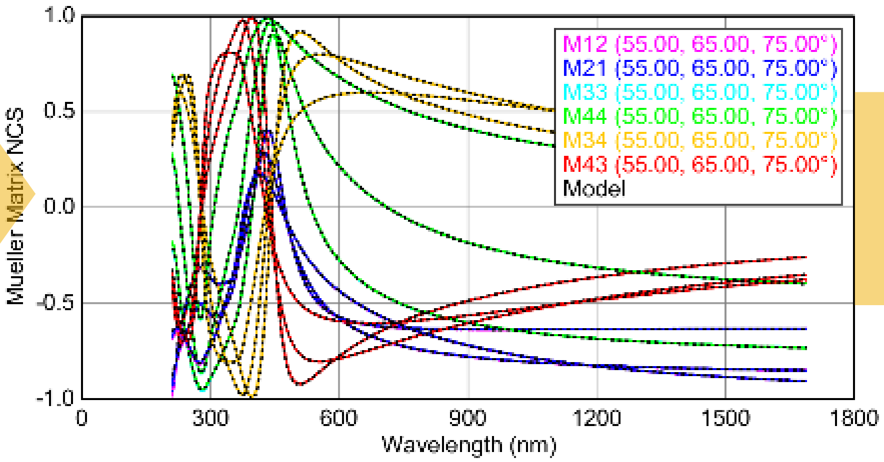

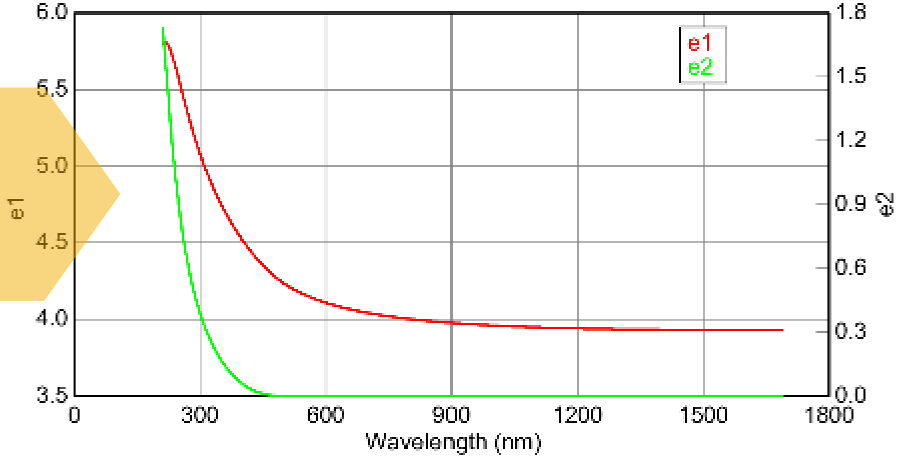

COLLEGE OF NANOTECHNOLOGY, SCIENCE, AND ENGINEERING
UNIVERSITY AT ALBANY | STATE UNIVERSITY OF NEW YORK

4X superlattice Si/Si(1-x)Ge(x) w/< 10nm films

- XRD thickness based fits improve MSE slightly compared to floating avg Si and SiGe SE fits
- EMA (Effective Medium Approximation) improves the fit by modeling the stack as a mix of Si and SiGe properties
- EDC (Effective Dielectric Constant) improved the model further by determining the dielectric constant for the layer set wavelength by wavelength

Superlattice Fit Strategy	Fix thk. based on XRD	Avg. Si and SiGe thk.	Superlattice EMA	Superlattice EDC
SiN Roughness [nm]	3.00	2.66	0.26	0.00
SiN Hardmask [nm]	47.96	47.90	48.23	48.30
Si [nm]	8.06	7.15		
Si(1-x)Ge(x) [nm]	6.74 (x=0.29)	6.08 (x=0.27)		
Si [nm]	8.02	7.15		
Si(1-x)Ge(x) [nm]	6.99 (x=0.27)	6.08 (x=0.27)	58.57	60.93
Si [nm]	8.12	7.15		
Si(1-x)Ge(x) [nm]	6.33 (x=0.27)	6.08 (x=0.27)		
Si [nm]	8.09	7.15		
Si(1-x)Ge(x) [nm]	6.55 (x=0.26)	6.08 (x=0.27)		
MSE	15.941	16.883	10.788	3.64

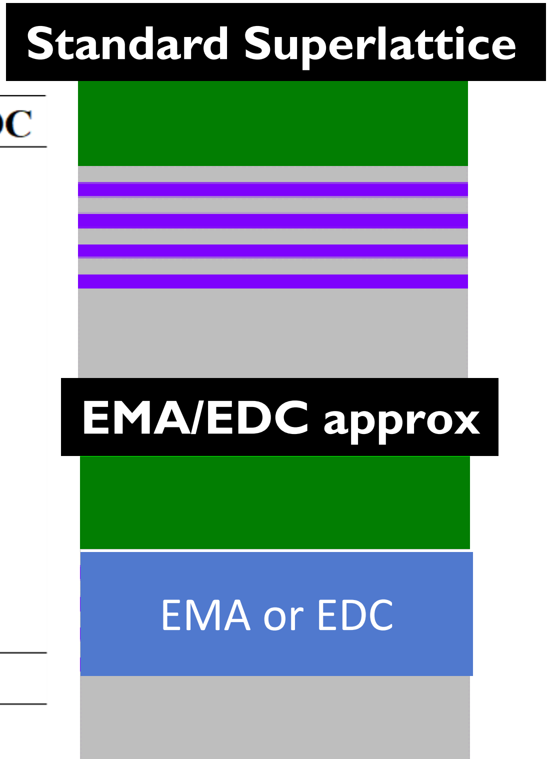

Optical Superlattice Effects
4X superlattice Si/Si(1-x)Ge(x) w/< 10nm films

- Extra absorption feature observed at 2.4 eV indicates the ***interfacial*** superlattice properties affect the effective dielectric constant (EDC)
- Observed broadening in 4-layer SL is similar to Attiaoui 2022 result

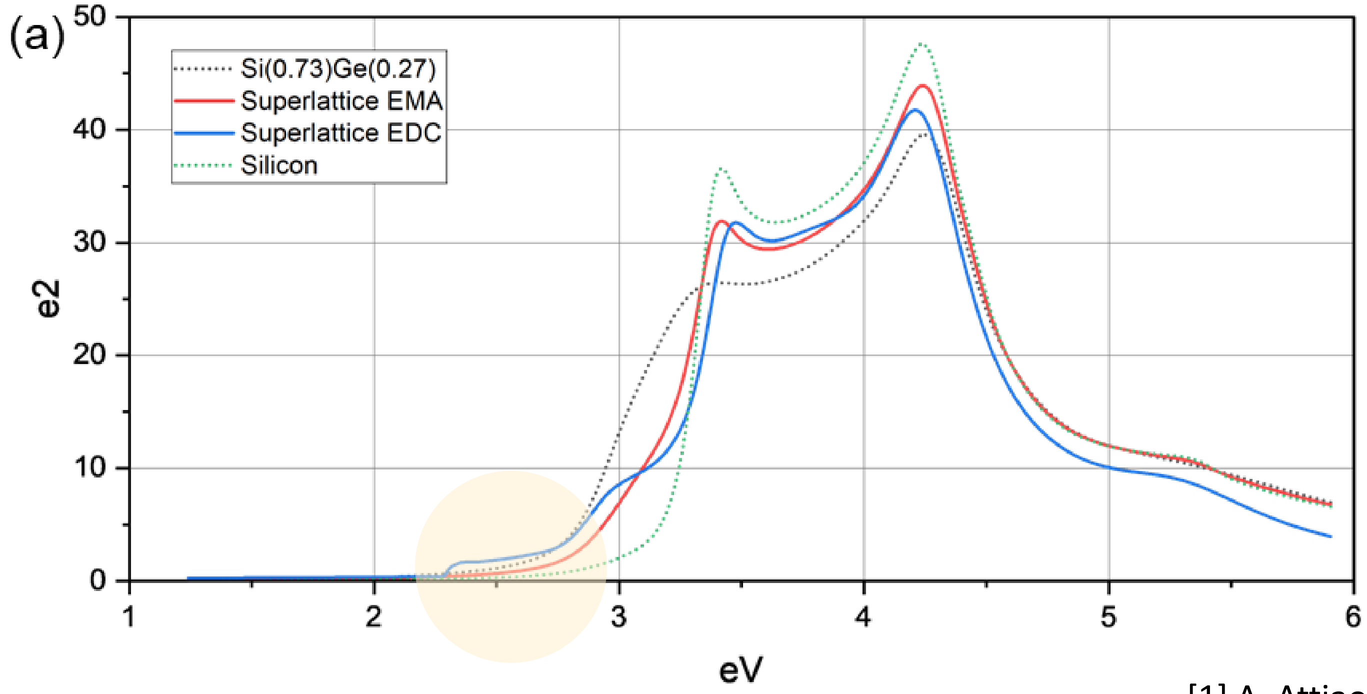

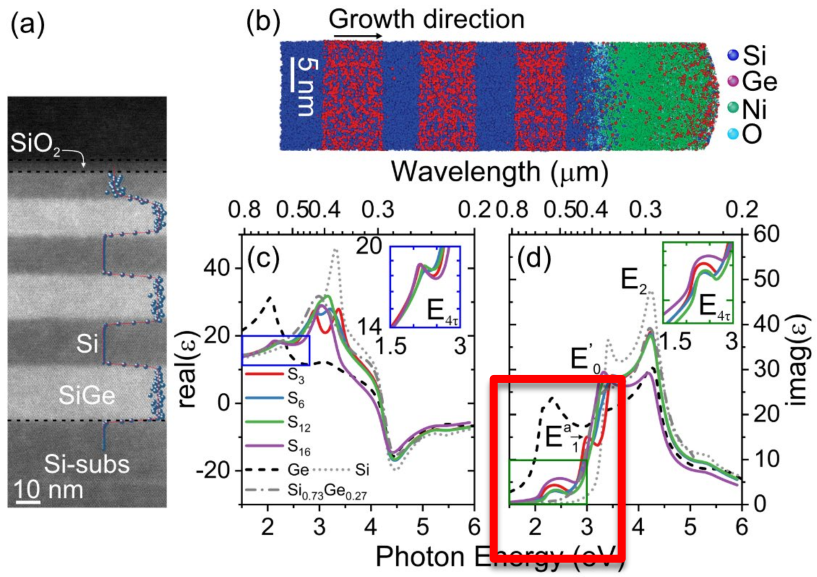

[1] A. Attiaoui et al., "Electronic Signature of Subnanometer Interfacial Broadening in Heterostructures," Nano Lett. **22**(17), 7080–7086 (2022) [doi:10.1021/acs.nanolett.2c02042].

Brillouin Zone Folding

Quasi-Direct Gap
~ 1 eV
in a superlattice does not have the same optical absorption when compared to those found in direct gap semiconductors such as GaAs.

Many layer superlattices may enhance absorption

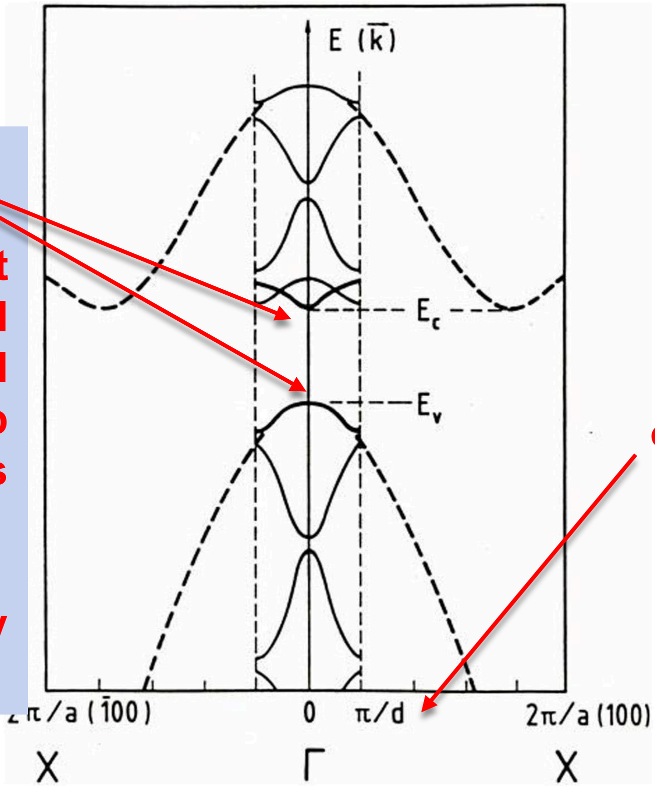

d is the superlattice periodicity

Schematic representation of the Brillouin zone-folding concept in Si resulting from the new superlattice periodicity in the growth direction.
Here, the conduction band minimum along the *X* direction is folded back into the Γ point when the superlattice period is about 10 monolayers of Si (Kasper and Schäffler, 1991).

Si/SiGe Heterointerfaces in One-, Two-, and Three-Dimensional Nanostructures: Their impact on SiGe Light emission
D.J. Lockwood, X. Wu, J-M Baribeau, S.A. Mala, X. Wang, and L. Tsybeskov, Frontiers in Materials, 2016 (doi: 10.3389/fmats.2016.00012)

Absorption Depth

- Absorption depth can be estimated using the Effective Medium Approximation model for Si/Si(0.75)Ge(0.25) based on
- Significant absorption of current 56 nm n=4 stacks occurs below 3 eV
- Absorption will be more significant for thicker future logic and 3D DRAM film stacks

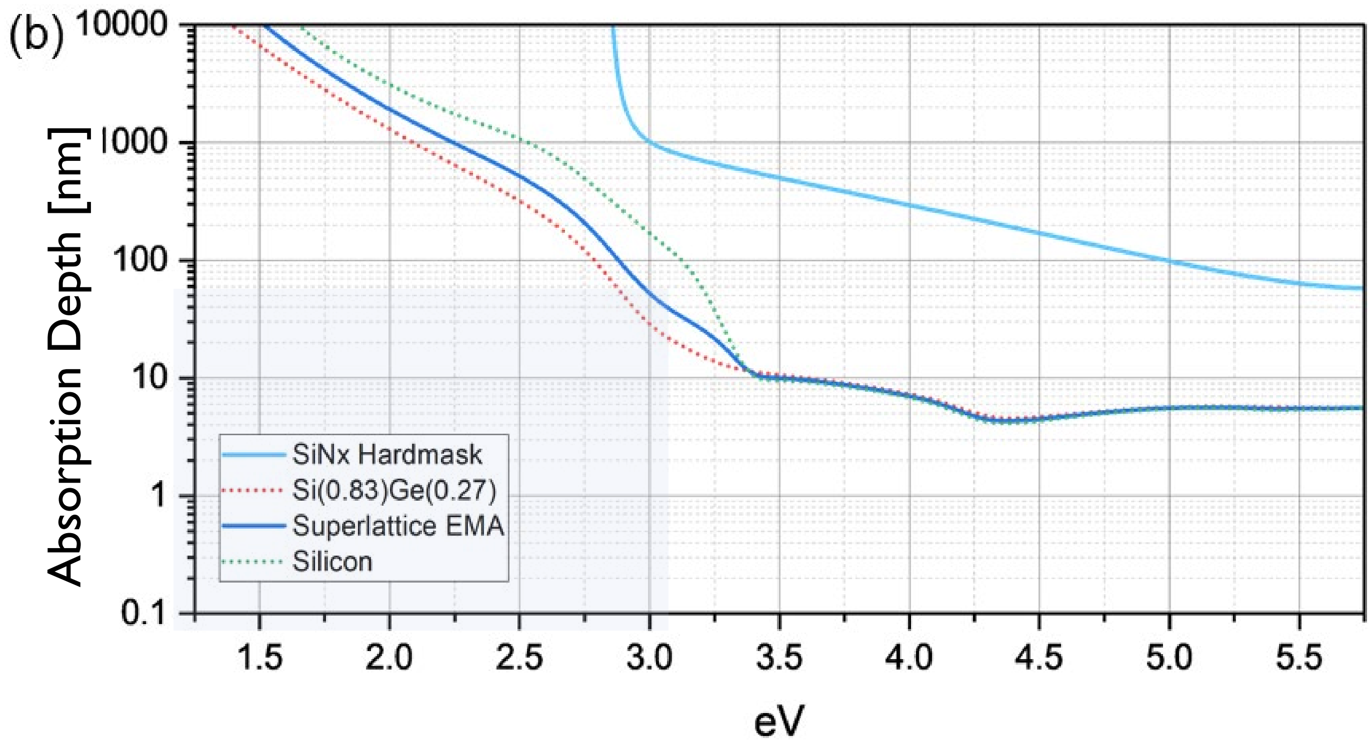

Standard Superlattice

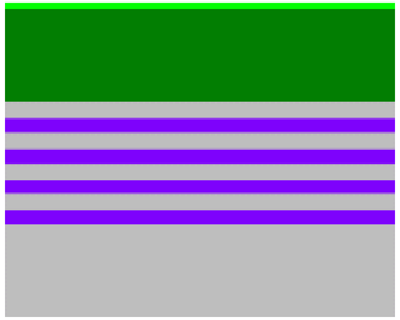

Effective Medium Approximation (EMA) Model

COLLEGE OF
NANOTECHNOLOGY,
SCIENCE, AND ENGINEERING
UNIVERSITY AT ALBANY | STATE UNIVERSITY OF NEW YORK

AGENDA

- What is Scatterometry & Requirements for Scatterometry
- 3D Structures, 3D Devices, and Nanoscale Materials
- X-Ray Characterization
- MMSE-Scatterometry
- 3D Nanowire Test Structures
- Conclusions

COLLEGE OF
NANOTECHNOLOGY,
SCIENCE, AND ENGINEERING
UNIVERSITY AT ALBANY | STATE UNIVERSITY OF NEW YORK

Gate All Around Transistor Process Flow

GAA Process Flow

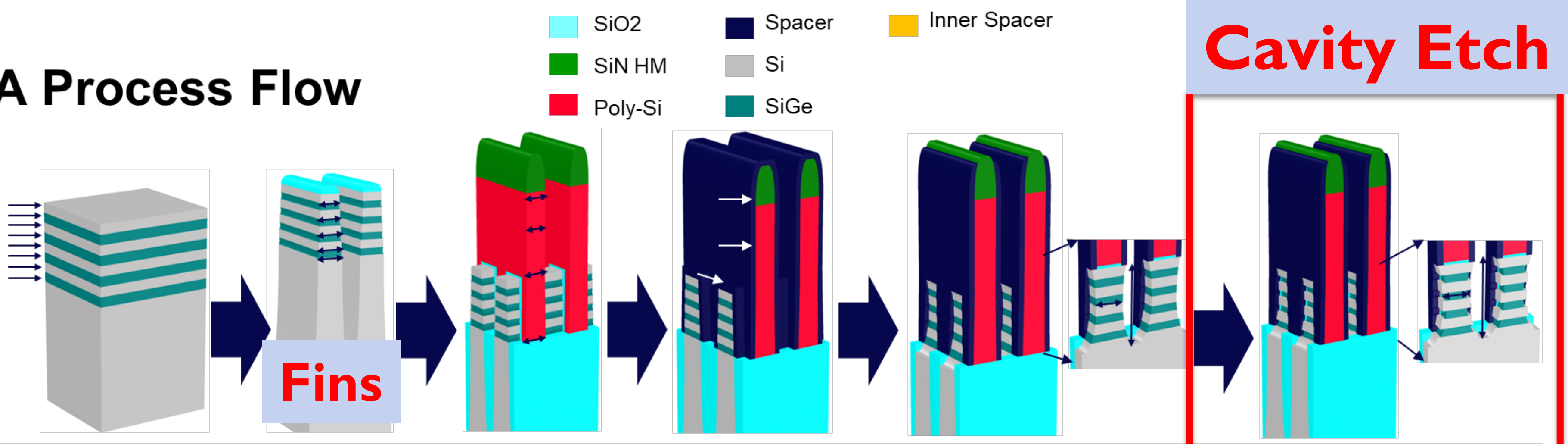

Step	Super Lattice Growth	Fin Etch	Gate Etch	Spacer Deposition	S/D Cavity Etch	SiGe Cavity Etch
Key Parameter(s)	Epi Thickness	Sidewall Profile	Gate Profile	Spacer Thickness	Cavity Proximity/Depth	SiGe Cavity Proximity/Depth

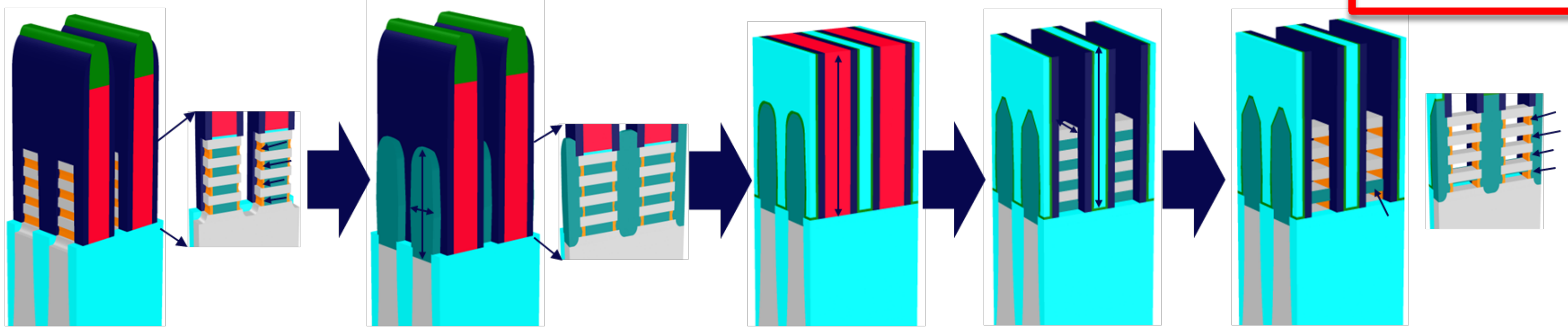

Inner Spacer Etch	Epi Growth	ILD Polish	Dummy Gate Removal	Channel Release
Inner Spacer CD (each NS)	Epi MCD/Height	Gate Height	Gate Height/NS Profile	SiGe Residual/Inner SPC CD

Nick Keller, ONTO Innovation, Nov. 2024

COLLEGE OF
NANOTECHNOLOGY,
SCIENCE, AND ENGINEERING
UNIVERSITY AT ALBANY | STATE UNIVERSITY OF NEW YORK

Nanowire Test Structure

Top view

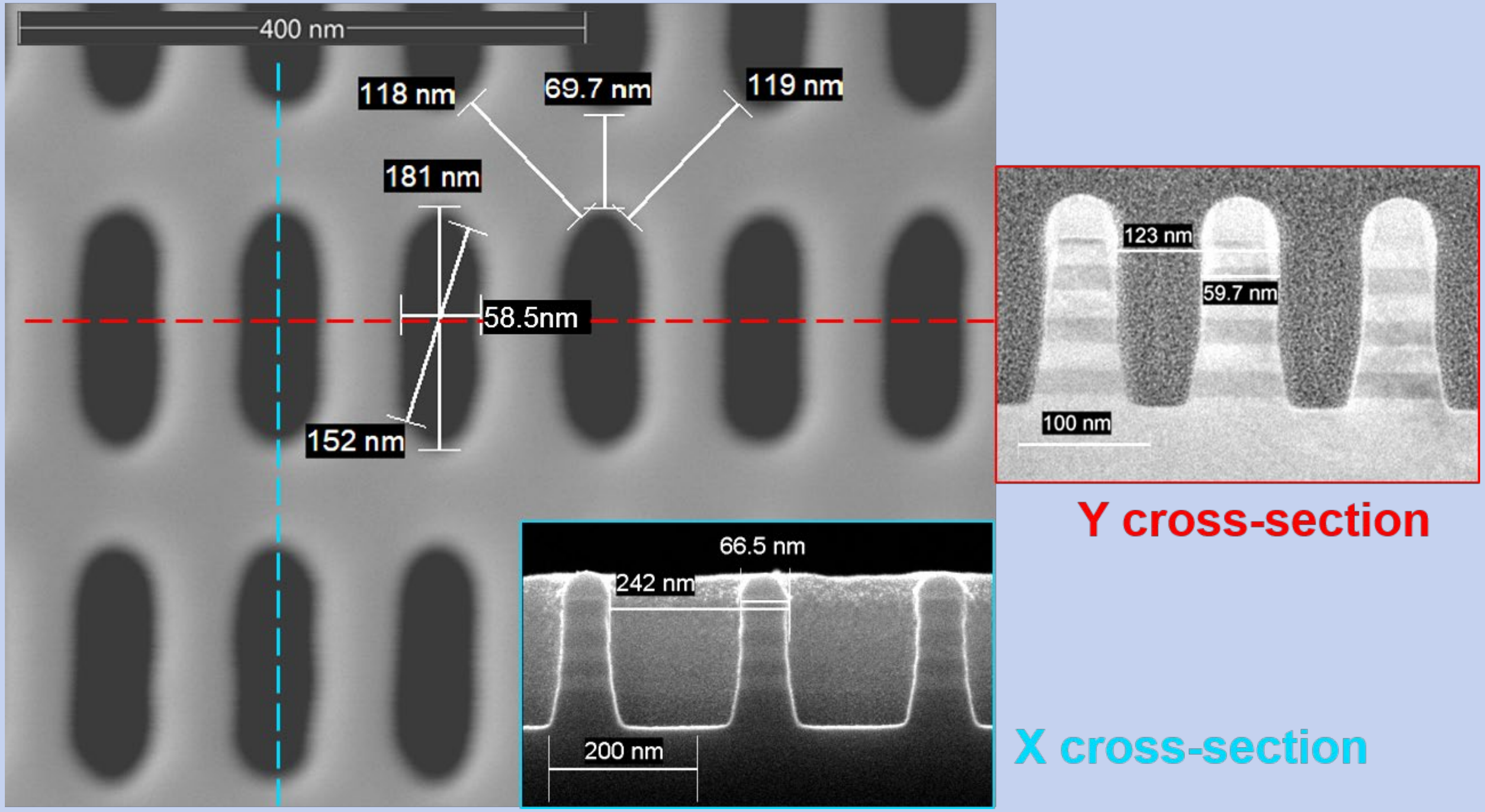

Y cross-section

X cross-section

Nanowire Test Structure

Nanowire Test Structures(NWTS) structure based on STEM

- Materials:
  - Si, SiGe (20% - 28% Germanium), SiN
- Parameters:
  - X pitch – 240nm
  - Y pitch – 120nm
- Hole dimensions:
  - 161.5nm*39.9nm at the bottom
  - 180nm*64.5nm at the top

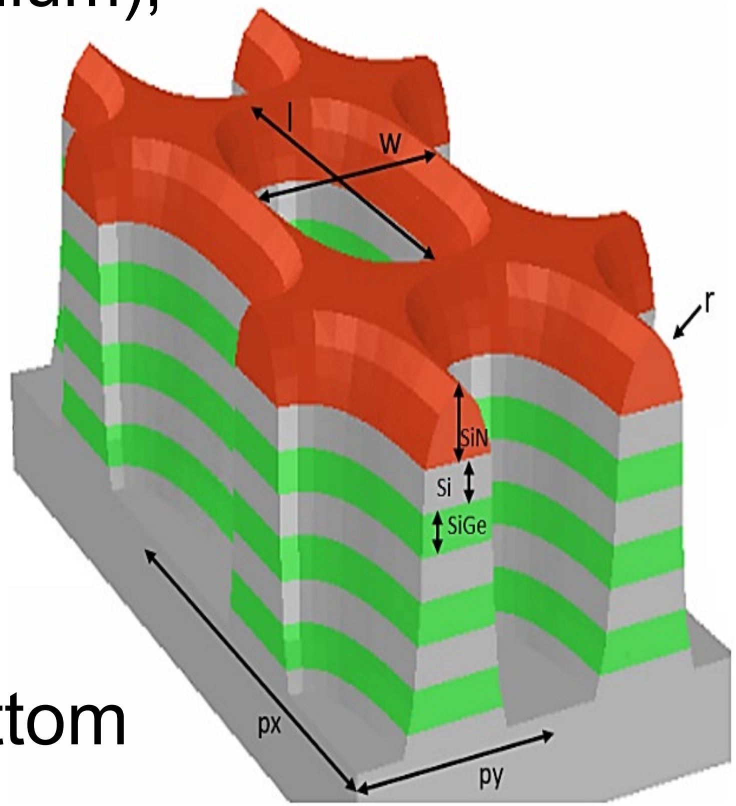

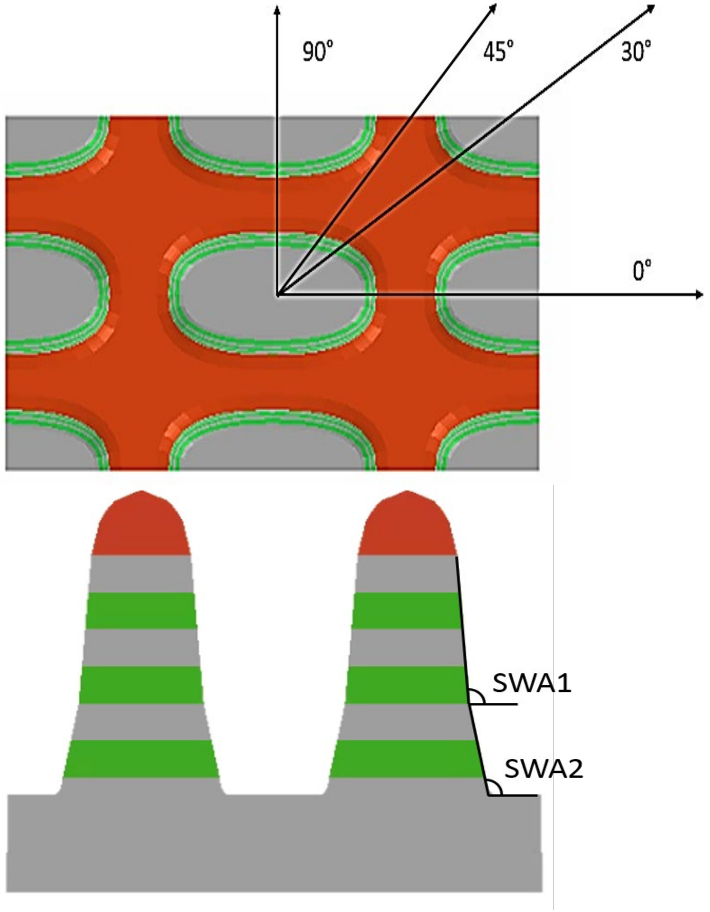

Polar plots: Comparison Etched vs Unetched

- Unetched Nanowire Test Structure

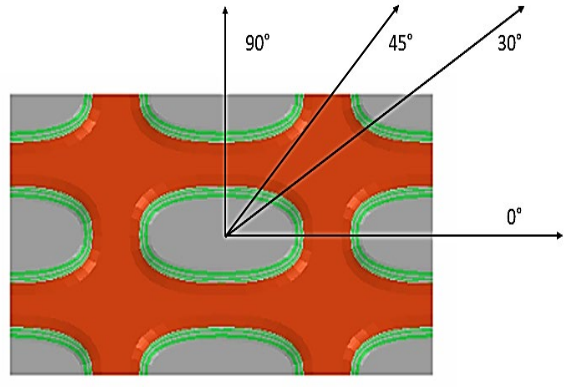

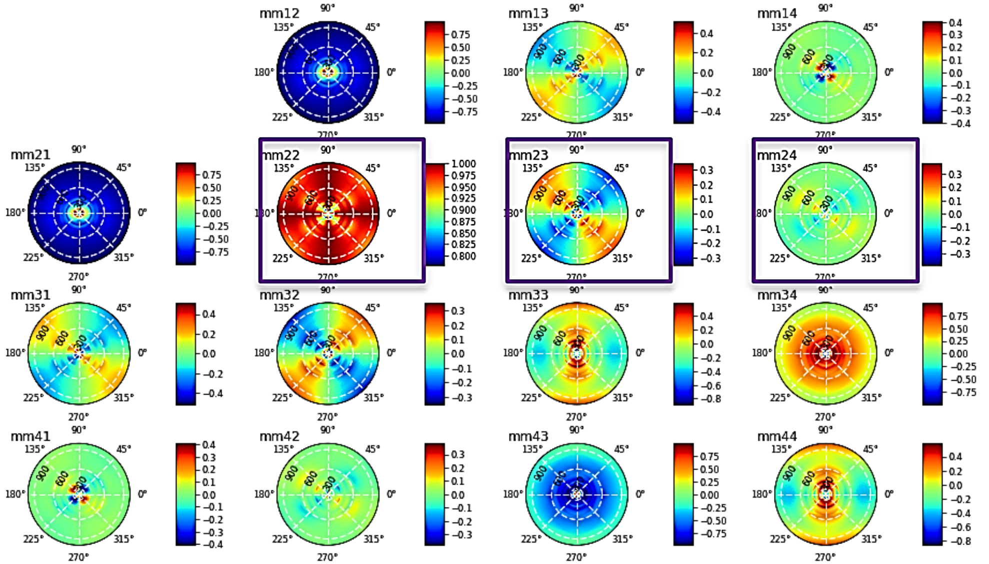

- Etched Nanowire Test Structure
  - (For a SiGe etch of 20 nm)
  - More sensitive MM Elements
  - More intricate features

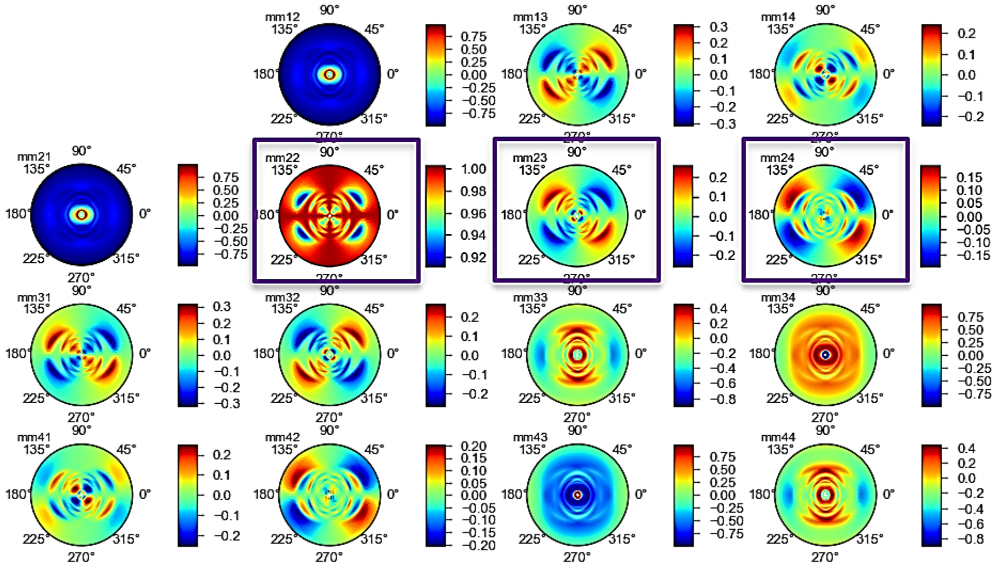

Asymmetric angles 30° and 45 have more symmetry

Experimental Sensitivity to SiGe layer etch aka : Cavity Etch

20 nm Si and SiGe layers

a

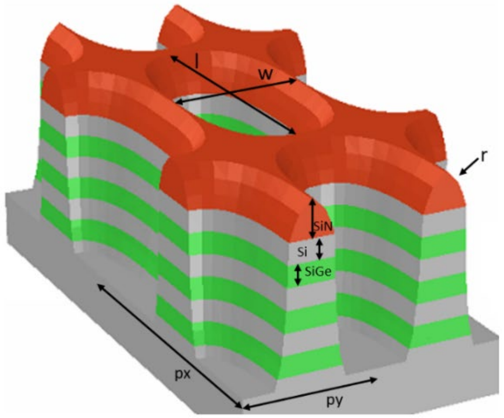

b

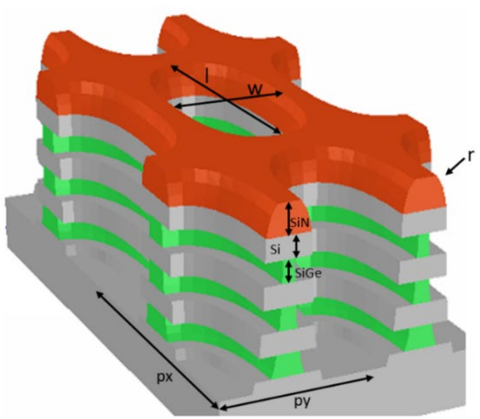

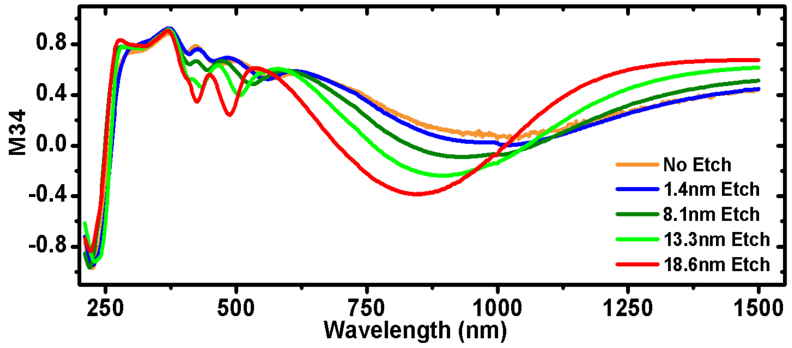

Selective etch analysis: Experimental data for MM34 at 45° azimuthal angle

Final Scatterometry model after fitting experimental data:

(a) Unetched Nanowire Test Structure after regression analysis

(a) Etched Nanowire Test Structure 10.5nm

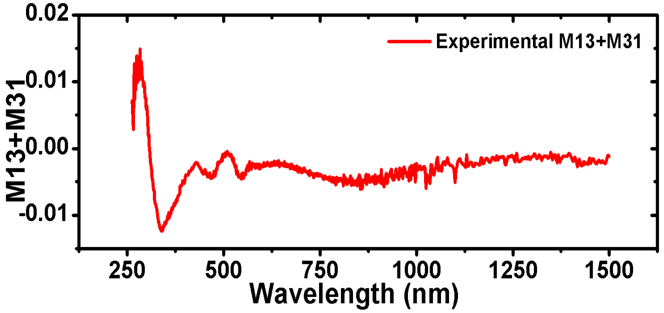

The residual value for M13+M31 for the 21.9 nm etched NWTS

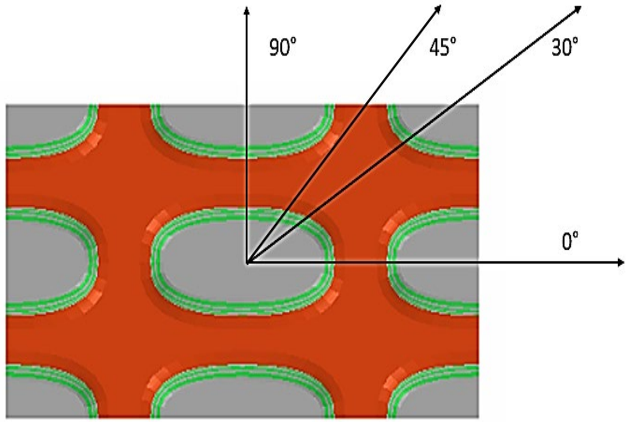

Experimental Sensitivity to SiGe layer etch

20 nm Si and SiGe layers

Average amount of selective etch of the SiGe layers from each side :

3.4nm 10.5nm 18.9nm 21.9nm

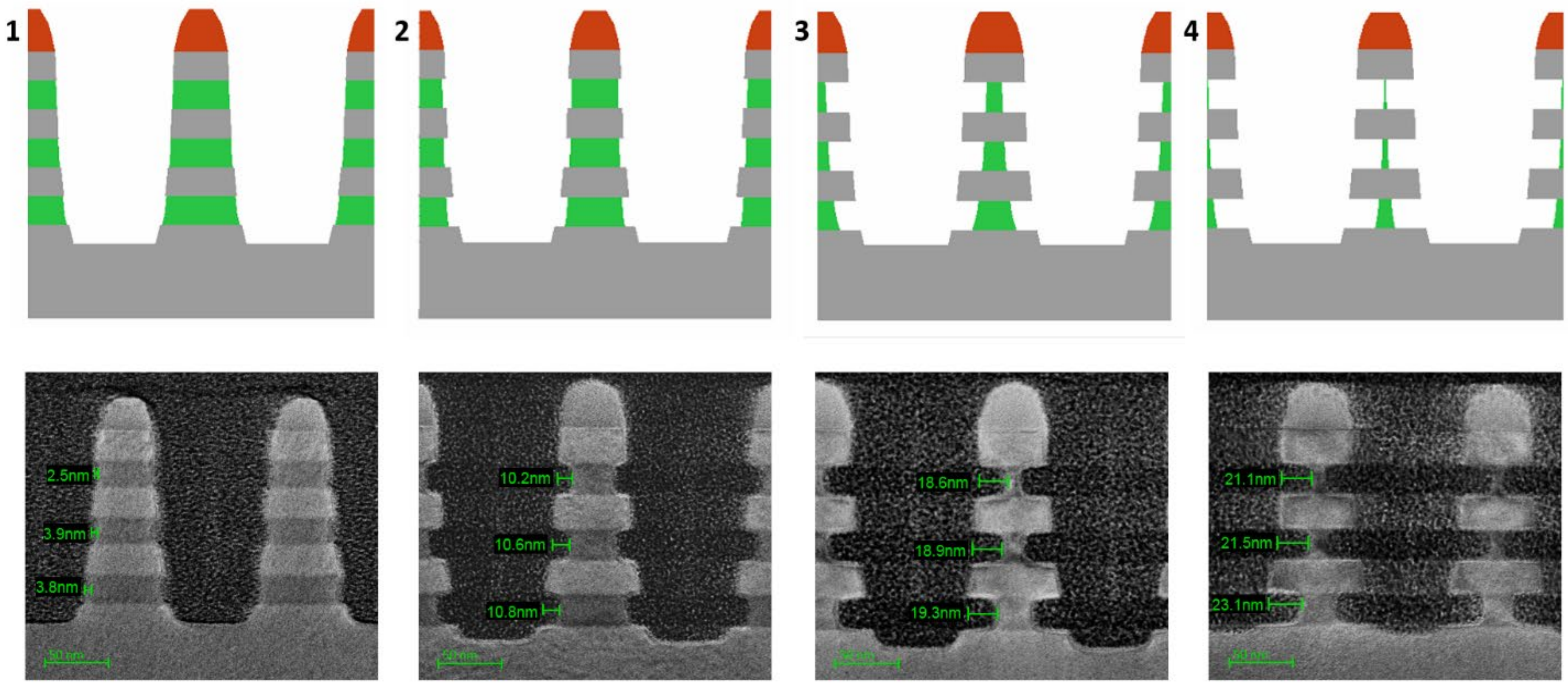

Y cross-sections

Selective etch of the SiGe layers in the NWTS

J. Vac. Sci. Technol. B, **38**, (2020), 024007.

Experimental Sensitivity to SiGe layer etch

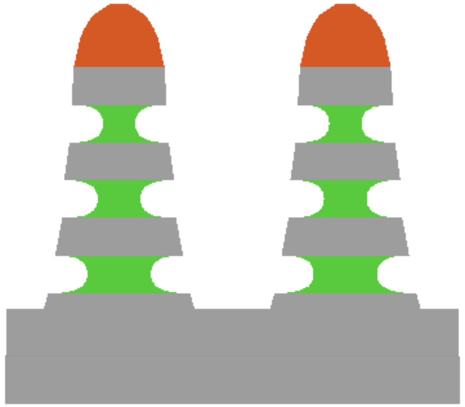

Curved Cavity Profile Model does not fit the 20 nm Si/ 20 nm Si(1-x)Ge(x) data.

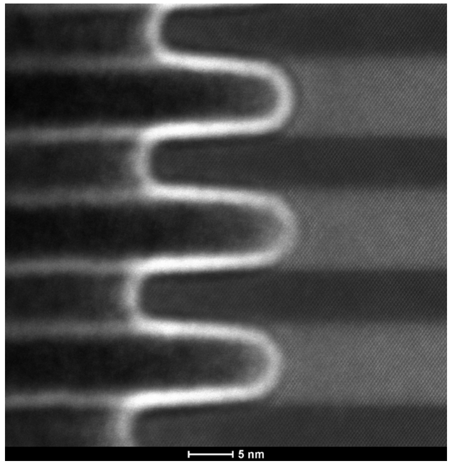

Curved Cavity Profile Model does fit the < 10 nm Si/< 10 nm Si(1-x)Ge(x) .

It also matches STEM images.

COLLEGE OF
NANOTECHNOLOGY,
SCIENCE, AND ENGINEERING
UNIVERSITY AT ALBANY | STATE UNIVERSITY OF NEW YORK

4x and 8x Superlattice NWTS

< 10 nm Si & Si(1-x)Ge(x) films

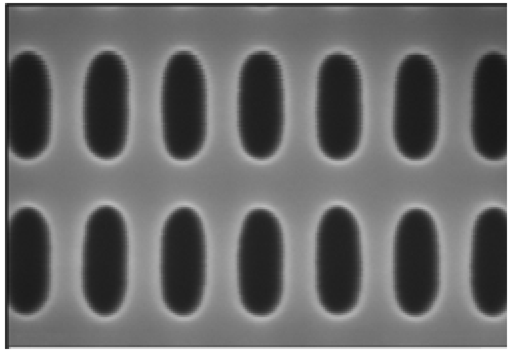

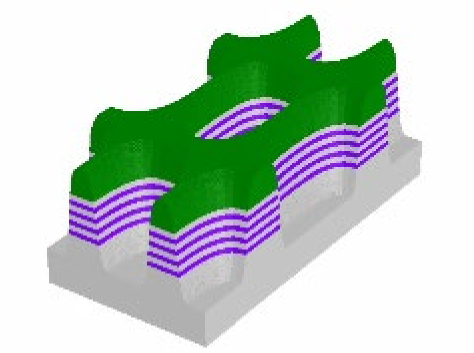

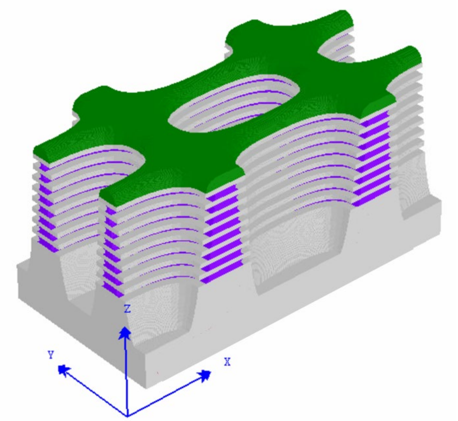

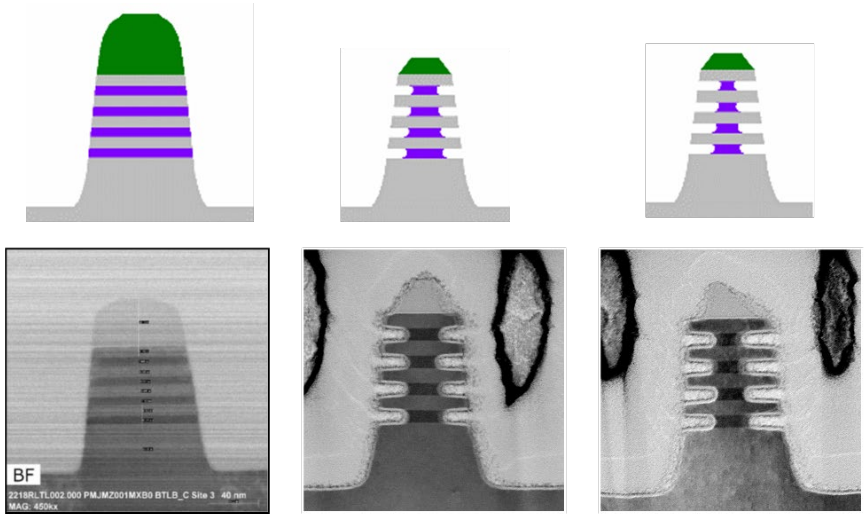

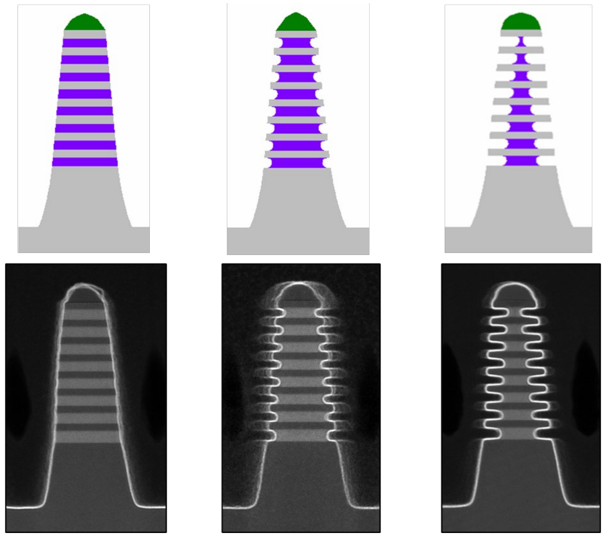

COLLEGE OF
NANOTECHNOLOGY, SCIENCE, AND ENGINEERING
UNIVERSITY AT ALBANY | STATE UNIVERSITY OF NEW YORK

STEM/EDS of 8X Superlattice

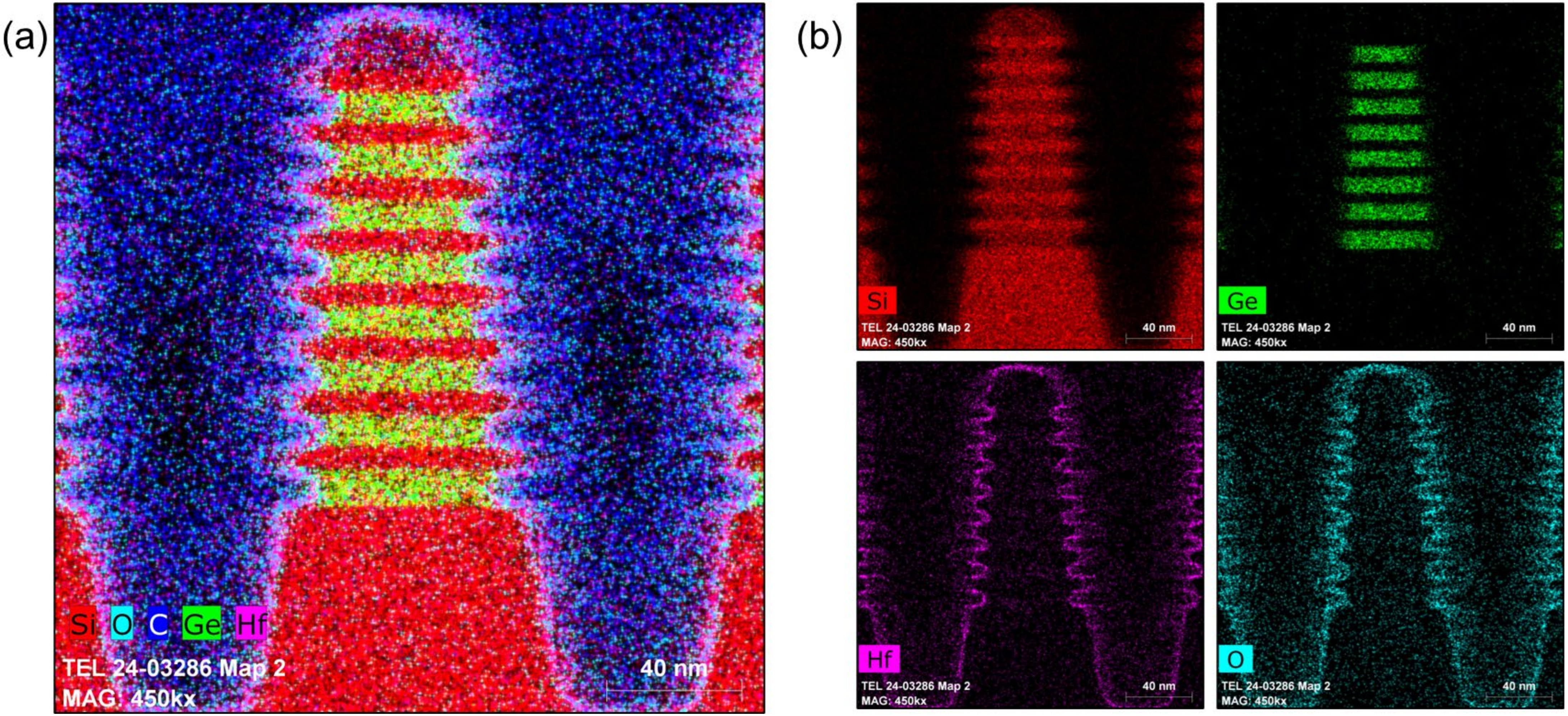

Critical Part of STEM -- Hf oxide protective coating before FIB sample preparation

8X superlattice Film Variation

Average HR-XRD Layer Thickness

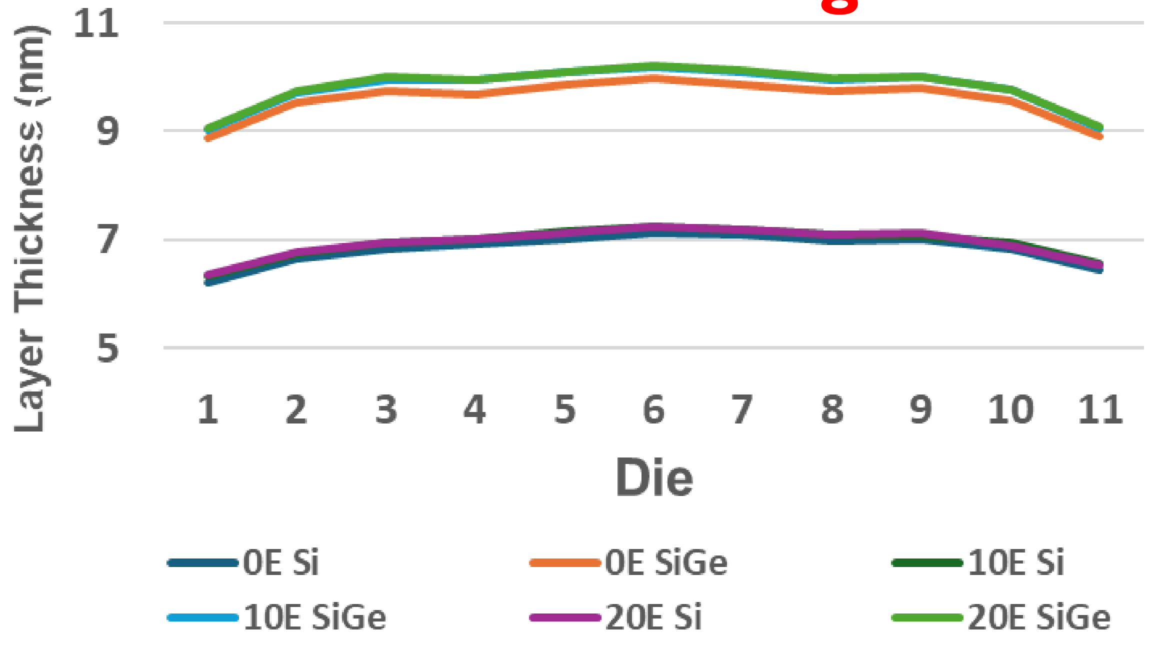

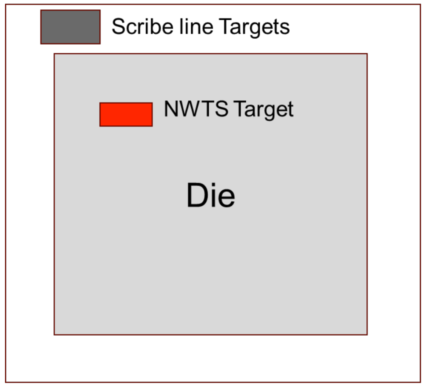

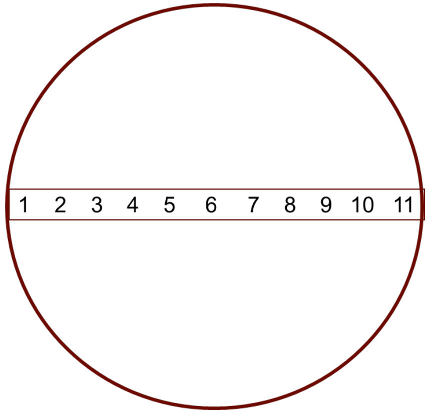

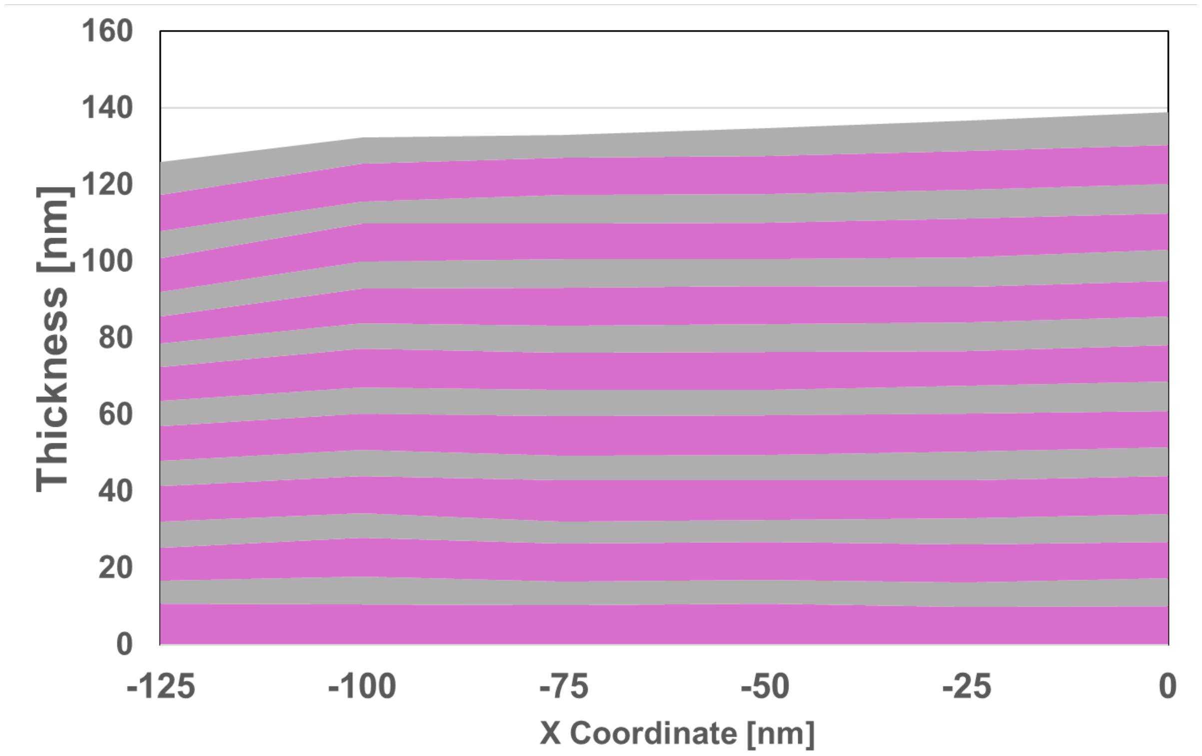

28.4 % Ge

COLLEGE OF NANOTECHNOLOGY, SCIENCE, AND ENGINEERING
UNIVERSITY AT ALBANY | STATE UNIVERSITY OF NEW YORK

STEM Cavity Etch Variation between layers Die 1

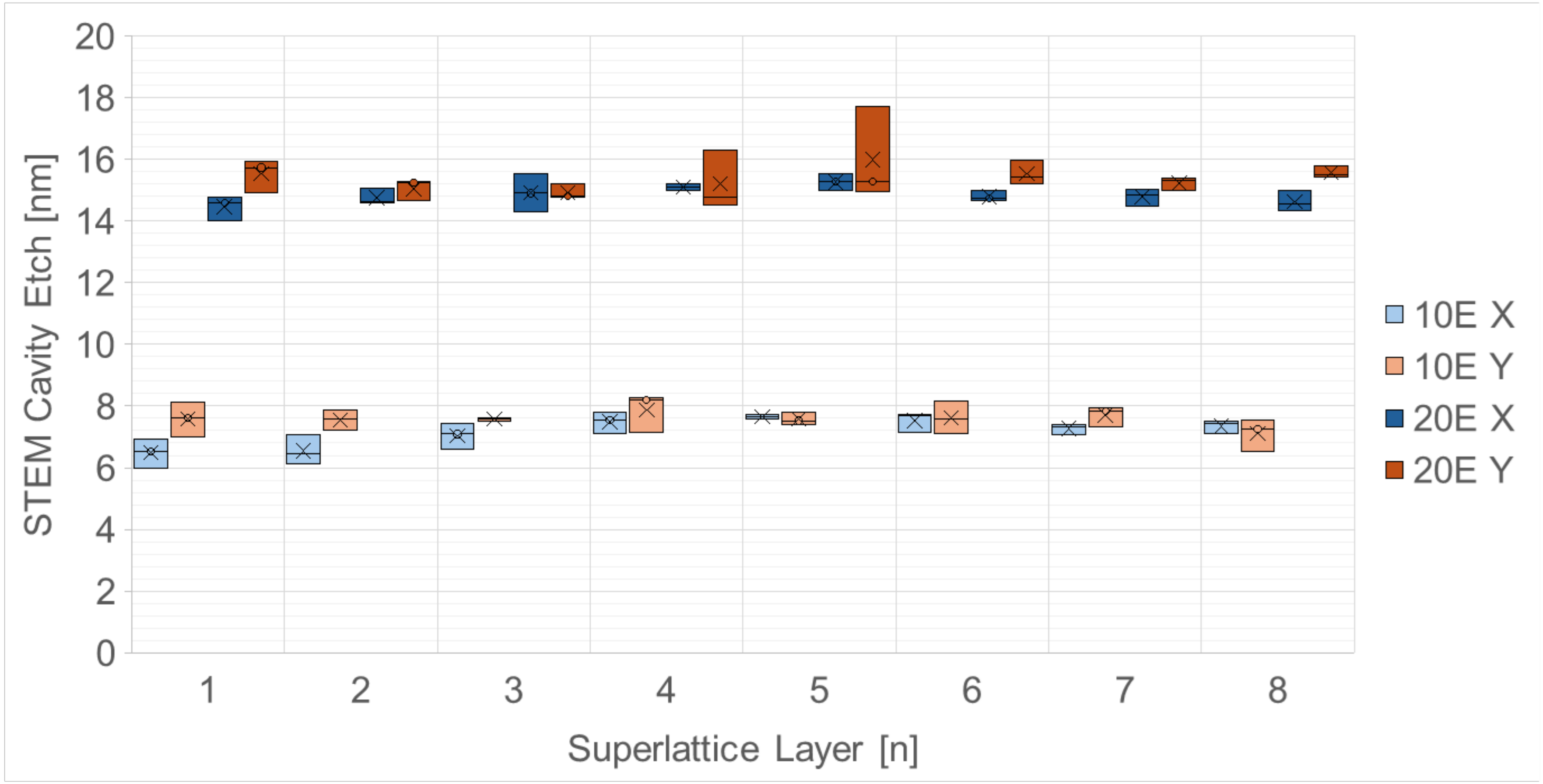

8X Superlattice Across-Wafer Variation

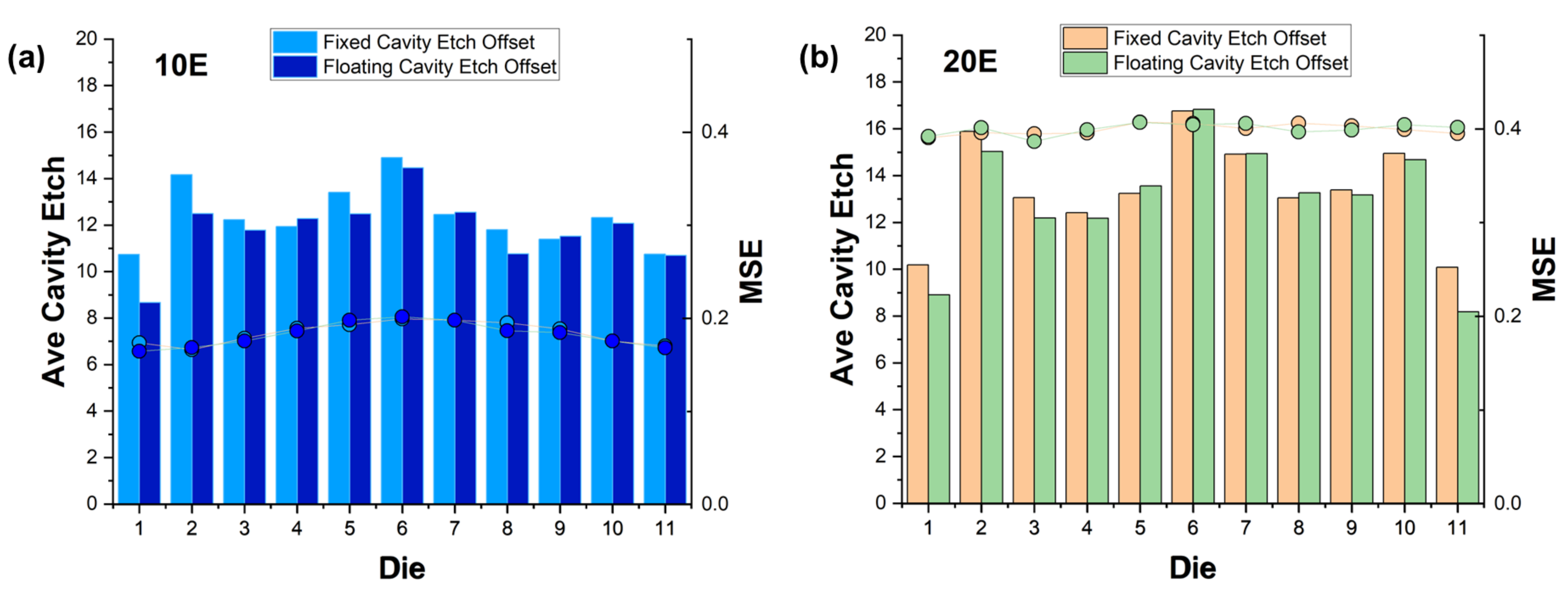

COLLEGE OF NANOTECHNOLOGY, SCIENCE, AND ENGINEERING
UNIVERSITY AT ALBANY | STATE UNIVERSITY OF NEW YORK

8X Superlattice : OCD vs STEM vs XRF

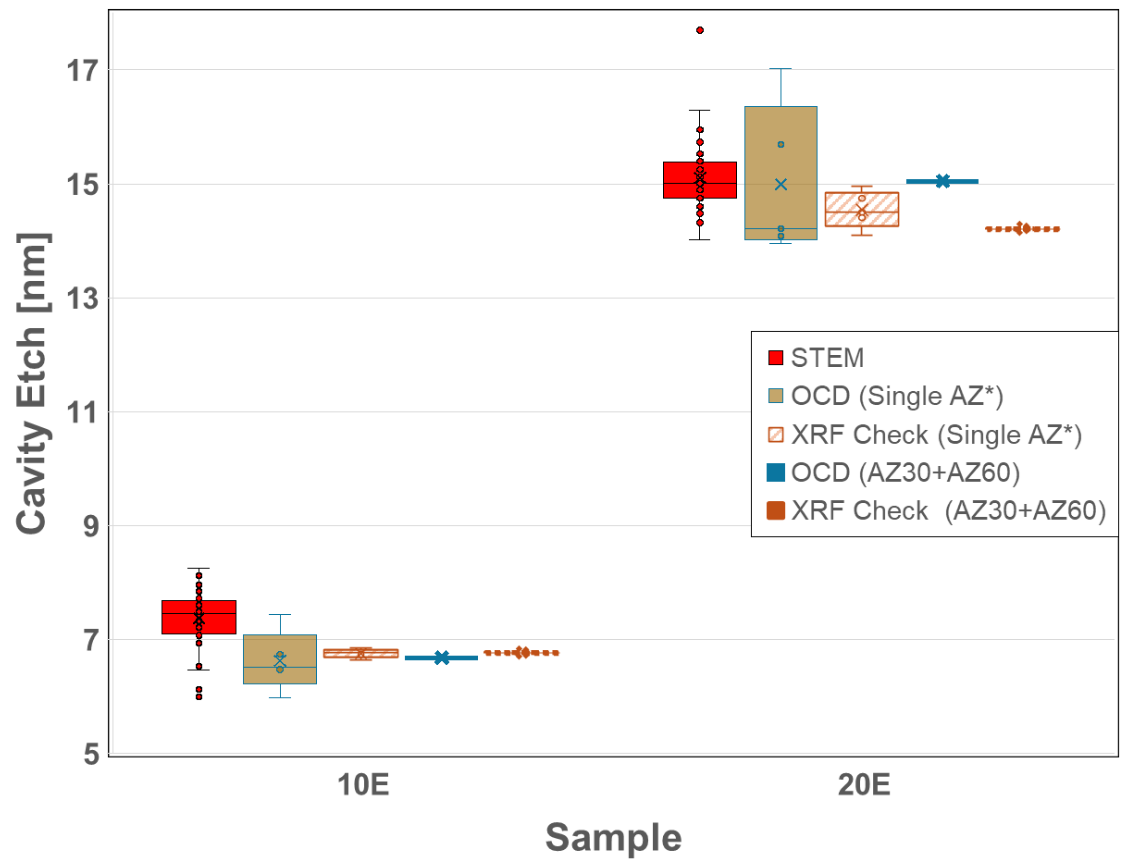

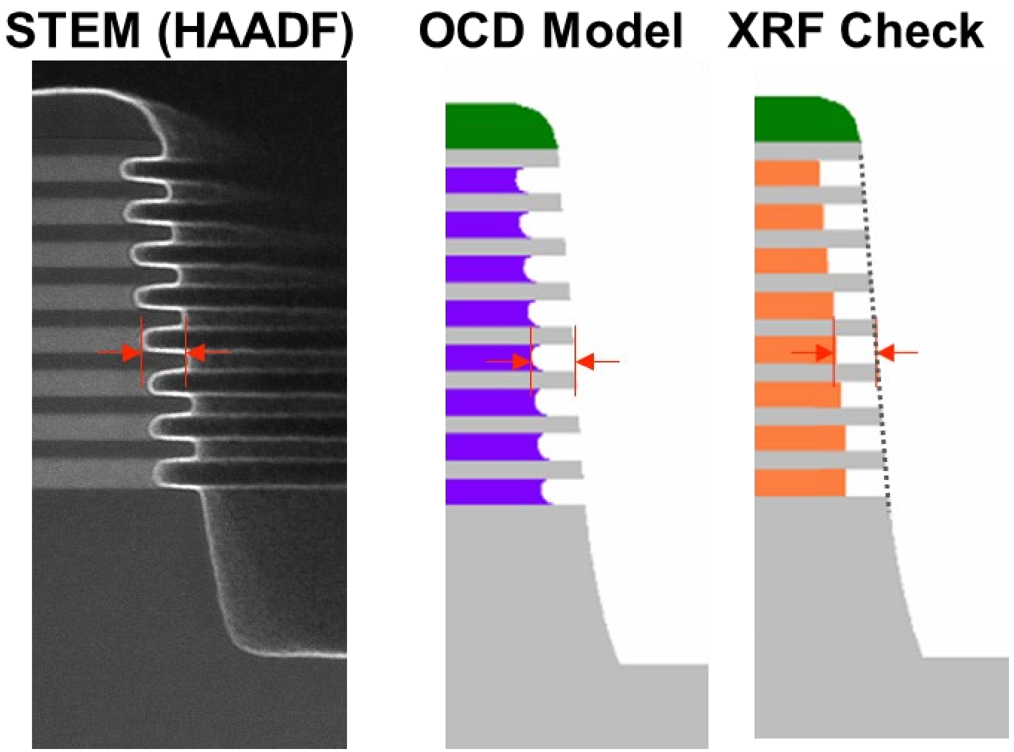

Sample	STEM	OCD (Single AZ*)	XRF Check (Single AZ*)	OCD (AZ30+AZ60)	XRF Check (AZ30+AZ60)
10E Avg. Cav. Etch [nm]	7.37	6.63	6.76	6.68	6.78
Δ = 10E Fit vs. STEM [nm]	--	*-0.74*	*-0.61*	*-0.69*	*-0.59*
20E Avg. Cav. Etch [nm]	**15.11**	**14.99**	**14.54**	**15.05**	**14.22**
Δ = 20E Fit vs. STEM [nm]	**--**	***-0.12***	***-0.56***	***-0.06***	***-0.89***

8X Superlattce Cavity Etch Correlation Tables

(a)

AZ30: Abs. Correlation

Y Tilt [deg]	1							High	0.9
X Tilt [deg]	0.56	1						Elevated	0.8
SWA [deg]	0.3	0.17	1					Low	0.5
Si Overetch [nm]	0.32	0.17	0.83	1					
Hole Width [nm]	0.27	0.08	0.04	0.22	1				
Hole Length [nm]	0.36	0.16	0.84	0.85	0.49	1			
Cavity Etch [nm]	0.18	0.08	0.87	0.73	0.02	0.79	1		
SiN Thk. [nm]	0.08	0.03	0.23	0.22	0.1	0.11	0.01	1	
SiN HM SWA [deg]	0.1	0	0.27	0.27	0.09	0.15	0.02	0.99	1
	Y Tilt [deg]	X Tilt [deg]	SWA [deg]	Si Overetch [nm]	Hole Width [nm]	Hole Length [nm]	Cavity Etch [nm]	SiN Thk. [nm]	SiN HM SWA [deg]

AZ60: Abs Correlation

Y Tilt [deg]	1							High	0.9
X Tilt [deg]	0.62	1						Elevated	0.8
SWA [deg]	0.26	0.1	1					Low	0.5
Si Overetch [nm]	0.31	0.19	0.7	1					
Hole Width [nm]	0.19	0.06	0.25	0.15	1				
Hole Length [nm]	0.33	0.09	0.69	0.79	0.45	1			
Cavity Etch [nm]	0.17	0.04	0.85	0.65	0.18	0.7	1		
SiN Thk. [nm]	0.08	0.02	0.22	0.14	0.26	0.07	0.04	1	
SiN HM SWA [deg]	0.09	0.01	0.22	0.15	0.26	0.07	0.05	0.99	1
	Y Tilt [deg]	X Tilt [deg]	SWA [deg]	Si Overetch [nm]	Hole Width [nm]	Hole Length [nm]	Cavity Etch [nm]	SiN Thk. [nm]	SiN HM SWA [deg]

(b)

AZ30+ AZ60: Abs. Correlation

Y Tilt [deg]	1							High	0.9
X Tilt [deg]	0.31	1						Elevated	0.8
SWA [deg]	0.06	0.02	1					Low	0.5
Si Overetch [nm]	0.04	0.03	0.76	1					
Hole Width [nm]	0.11	0.04	0.33	0.21	1				
Hole Length [nm]	0.12	0.01	0.84	0.7	0.12	1			
Cavity Etch [nm]	0.05	0.06	0.75	0.59	0.5	0.6	1		
SiN Thk. [nm]	0.07	0.11	0.19	0.32	0.24	0.02	0.06	1	
SiN HM SWA [deg]	0.07	0.08	0.23	0.34	0.2	0.06	0.02	0.99	1
	Y Tilt [deg]	X Tilt [deg]	SWA [deg]	Si Overetch [nm]	Hole Width [nm]	Hole Length [nm]	Cavity Etch [nm]	SiN Thk. [nm]	SiN HM SWA [deg]

AGENDA

- What is Scatterometry & Requirements for Scatterometry
- 3D Structures, 3D Devices, and Nanoscale Materials
- X-Ray Characterization
- MMSE-Scatterometry
- 3D Nanowire Test Structures
- Conclusions

Conclusions

- **HYBRID Metrology –**
  - X-Ray methods provide key information about superlattice structures
  - STEM provides feature dimensional reference
- (for ~ 6 layer superlattice) Superlattice effect on optical properties due to interfacial layer (or roughness) not due to Brillouin zone folding.
- Mueller Matrix Spectroscopic Ellipsometry enables scatterometry of complex structures
- MMSE-scatterometry is capable of non-destructively measuring sub-surface etching of complicated 3D structures --- Requires individual layer optical properties for etched SiGe

Some References

- E. Pasikatan, C. Wadsworth, N. Keller, G.A. Antonelli, A.C. Diebold. Characteristic Mueller matrix responses and correlation analysis for vertical GAA nanowire structure manufacturing using RCWA simulated spectra, submitted.
- E. Pasikatan, G.A. Antonelli, N. Keller, S. Kal, M. Rednor, K. Tapily, D. Hetzer, M. Schaefer, M. Kuhn, S. Murakami, and A.C. Diebold, Superlattice effects and limitations of non-destructive measurement of advanced Si/Si1−xGex superlattice structures using Mueller matrix scatterometry and high-resolution X-ray diffraction, J. Micro/Nanopattern. Mater. Metrol. 23, (2024), 044004.
- Non-destructive characterization of nanoscale sub-surface features during selective etching of multi-layered Nanowire Test Structures using Mueller Matrix Spectroscopic Ellipsometry based scatterometry, M. Korde, S. Kal, C. Alix, N. Keller, G.A. Antonelli, A. Mosden, A.C. Diebold, J. Vac. Sci. Technol. B, **38**, (2020), 024007.
- Perspective: Optical measurement of feature dimensions and shapes by scatterometry, A.C. Diebold, A. Antonelli, N. Keller, APL Mat. **6**, (2018), 058201. doi: 10.1063/1.5018310.
- Optical CD Metrology for Directed Self-Assembly Assisted Contact Hole Shrink, D.J. Dixit, A. Green, E.R. Hosler, V. Kamineni, M. Preil, N. Keller, J. Race, J.S. Chun, M. O'Sullivan , P. Khare, W. Montgomery, A.C. Diebold, Journal of Micro/Nano Lithography, MEMS & MOEMS 15(1), (2016), 014004.
- Utilizing Tunable Absorption Properties of Light for Enhanced Ellipsometry of Metal Gratings, S. O'Mullane, Nick Keller, J. Race, A.C. Diebold, Journal of Micro/Nano Lithography, MEMS & MOEMS 15, (2016), 044003.

Some References

- Sensitivity Analysis and LER Determination of 28 nm Pitch Silicon Fins using Mueller Matrix Spectroscopic Ellipsometry based Optical CD Metrology, D. Dixit, S. O'Mullane, S. Sunkoju, A. Gottipati, E.R. Hosler, V. Kamineni, M. Preil, N. Keller, J. Race, G. R. Muthinti, A.C. Diebold, Alternative Lithographic Technologies IV, Journal of Micro/Nano Lithography, MEMS & MOEMS **14**, (2015), 031208.
- Metrology for Block Copolymer Directed Self-Assembly Structures using Mueller Matrix based Scatterometry, D. J. Dixit, V. Kamineni, R. Farrell,, E. R. Hosler,, M. Preil, J. Race, B. Peterson, A. C. Diebold, Control of IC Patterning Variance. Part 1: Metrology, Process Monitoring, and Control of Critical Dimension in Journal of Micro/Nano Lithography, MEMS & MOEMS **14**, (2015), 021102.
- Enhancing One Dimensional Sensitivity with Plasmonic Coupling, S. O'Mullane, B. Peterson, J. Race, N. Keller, A.C. Diebold, Optics Express 22, (2014), 26247. Erratum Optics Express **24**, (2016) 3613.
- The optical properties of pseudomorphic Ge(1-x)Snx (x = 0 to 0.11) alloys on Ge(001), M. Medikonda, G. R. Muthinti, R. Vasic, T. Adam, A. Reznicek, M. Wormington, G. Malladi and A.C. Diebold, J. Vac. Sci. Technol. B 32, (2014) 061805 (2014).
- Measurement of Periodicity and Strain in Arrays of Single Crystal Silicon and Pseudomorphic $Si_{1-x}Ge_x$/Si Fin Structures using X-ray Reciprocal Space Maps, M. Medikonda, G. Muthinti, J. Fronheiser, V. Kamineni, M. Wormington, K. Matney, T. Adam, E. Karapetrova and A.C. Diebold, J. Vac. Sci. Technol. B32, (2014), 021804.
- Effects of stress on the dielectric function of strained pseudomorphic $Si_{1-x}Ge_x$ alloys from 0 to 75 % Ge grown on Si (001) G.R. Muthinti, M. Medikonda, T.N. Adam, A. Reznicek, and A.C. Diebold, J. Appl. Phys. **112**, (2012), 053519.

Some Conference Proceedings

- Hybrid metrology for non-destructive lateral cavity etch measurements of 8-superlattice layer nanowire test structures (NWTS) using optical Mueller Matrix Spectroscopic Ellipsometry (MMSE) and X-ray Diffraction (XRD) and X-ray Reflectivity (XRR), E. Pasikatana, G.A. Antonelli, N. Keller, S. Kal, M. Rednor, K. Tapily, D. Hetzer, M. Schaefer, M. Kuhn, S. Murakami, A.C. Diebold, Metrology, Inspection, and Process Control XXXIX, San Jose, Feb.24-27, 2025.
- Superlattice Effects and limitations of non-destructive measurement of advanced Si/Si1-x Gex superlattice structures using Mueller Matrix Scatterometry (MMSE) & High-Resolution X-Ray Diffraction (XRD), E. Pasikatan, G.A. Antonelli, N. Keller S. Kal, M. Rednor, Markus Kuhn, A.C. Diebold, Metrology, Inspection, and Process Control XXXVIII, San Jose,Feb.26-29, 2024.
- Characteristic Mueller matrix responses and correlation analysis for vertical GAA nanowire structure manufacturing using RCWA simulated spectra, C. Wadsworth, E. Pasikatan, N. Keller, A. Antonelli, A.C. Diebold, " Proc. SPIE 12496, Metrology, Inspection, and Process Control XXXVII, 1249619 (27 April 2023); doi: 10.1117/12.2657690.
- Scatterometry of nanowire/nanosheet FETs for advanced technology nodes, M. Korde, S. Kal, C. Alix, N. Keller, G. A. Antonelli, A. Mosden, and A.C. Diebold, Metrology, Inspection, and Process Control for Semiconductor Manufacturing XXXV, edited by Ofer Adan, John C. Robinson, Proc. of SPIE Vol. 11611, (2021), 116111S.

Some Conference Proceedings

- Metrology for Advanced Transistor and Memristor Devices and Materials, A.C. Diebold and N. Cady, Proceedings of SPIE Advanced Lithography: Metrology, Inspection, and Process Control for Microlithography XXXIII, Proc. of SPIE Vol. 11325 (2020), 1132502.
- *The SPIE Diana Nyyssonen Memorial Best Paper Award 2020/21 Winner:* X-ray metrology of nanowire/ nanosheet FETs for advanced technology nodes, Madhulika Korde, R. Joseph Kline, Daniel F. Sunday, Nick Keller, Subhadeep Kal, Cheryl Alix, Aelan Mosden, Alain C. Diebold, Proceedings Volume 11325, Metrology, Inspection, and Process Control for Microlithography XXXIV, (2020), 113250W.

Book Chapters

- Advanced Ellipsometry Measurements for Semiconductor Structures, S.J. O'Mullane, D. Dixit, and A.C. Diebold, Characterization and Metrology for Nanoelectronics and Nanostructures, (Pan Stanford, 2016), Chapter 3.

- Spectroscopic Ellipsometry of Nanoscale Materials for Semiconductor Device Applications, A.C. Diebold, F.J. Nelson, and V.K. Kamineni, Ellipsometry at the NanoScale, (Springer, Berlin, 2013), Chapter 16.